



Modelling decadal trends and the impact of extreme events on carbon fluxes in a deciduous temperate forest using the QUINCY model

Tea Thum¹, Tuuli Miinalainen¹, Outi Seppälä¹, Holly Croft², Cheryl Rogers³, Ralf Staebler⁴, Silvia Caldararu⁵, and Sönke Zaehle⁶

¹Finnish Meteorological Institute, P.O. Box 503, 00101 Helsinki, Finland

²University of Sheffield, Western Bank, Sheffield S10 2TN, The United Kingdom

³Toronto Metropolitan University, Jorgenson Hall, 350 Victoria Street Toronto, ON M5B 2K3, Canada

⁴Environment and Climate Change Canada, 867 Lakeshore Rd Burlington ON L7S 1A1, Canada

⁵Trinity College, College Green, Dublin 2, Ireland

⁶Max Planck Institute for Biogeochemistry, Hans-Knöll-Straße 10, 07745 Jena, Germany

Correspondence: Tea Thum (tea.thum@fmi.fi)

Abstract. Changing climatic conditions pose a challenge to accurately estimate the carbon sequestration potential of terrestrial vegetation, which is often mediated by Nitrogen availability. The close coupling between the Nitrogen and Carbon cycles controls plant productivity and shapes the structure and functional dynamics of ecosystems. However, how carbon and nitrogen interactions affect both carbon fluxes and plant functional traits in dynamic ecotones, which are experiencing disturbance and species compositional shifts remains unclear. In this work, we use in-situ measurements of leaf chlorophyll content (Chl_{Leaf} , years 2013-2016) and leaf area index (LAI, years 1998-2018) to parameterise the seasonal dynamics of the QUINCY ('QUantifying Interactions between terrestrial Nutrient CYcles and the climate system') terrestrial biosphere model (TBM) to simulate the carbon fluxes at the Borden Forest Research Station flux tower site, Ontario, Canada, over 22 years from 1996-2018. QUINCY was able to simulate leaf-level maximum carboxylation capacity ($V_{c(max),25}$), Chl_{Leaf} and leaf nitrogen quite consistent with observations. The improved model captured observed daily gross primary production (GPP) well ($r^2=0.80$). Nevertheless, we found that although observed GPP increased significantly during the study period, and NEE shifted towards a stronger sink, these trends were not captured in the model. Instead, QUINCY showed a significant increasing trend for total ecosystem respiration (TER), that was not present in the observations. The severe drought in 2007 affected observed carbon fluxes strongly, lowering both GPP and TER also in the following year. QUINCY was able to capture some of the decrease in GPP and TER in 2007. However, the legacy effect of the drought in 2008 was not captured by the model. These results call for further work on representing legacy effects in TBMs, as these can have long-lasting impacts on ecosystem functioning.



1 Introduction

Climate change impacts the exchange of carbon (C), water and energy between vegetation and the atmosphere, as well as the
20 biogeochemical cycles and carbon storage potential of the ecosystems (Canadell et al., 2022). The C and nitrogen (N) cycles
are closely interconnected, with N a significant component of plants and a vital macronutrient. N is required for growth, de-
velopment and metabolic processes, and is a fundamental constituent of DNA and various plant structural and photosynthetic
components, such as light harvesting complexes and the electron transport chain (ETC). Additionally, it is an integral compo-
nent of many enzymes involved in the Calvin cycle. N deficit therefore limits photosynthesis, which ultimately decreases plant
25 productivity (LeBauer and Treseder, 2008). The future carbon pools and budgets in the coming decades depend, in part, on the
N cycle and availability of N to vegetation (Arora et al., 2020; Huntingford et al., 2022; Zaehle, 2013).

At large spatial scales, satellite observations have shown longer growing seasons in deciduous forests that has been attributed
to warming temperatures, although the rate of change has slowed (Fu et al., 2015; Piao et al., 2019a). A particularly important
aspect of long-term observations are the anomalous years or events. It is crucial to use these data to assess the ability of the
30 models to capture these anomalies and their impact on the vegetation functioning, as extreme events are predicted to become
more frequent. Drought is one of the most important stressors from the extreme events that can have profound effects on the
carbon cycle (Piao et al., 2019b). Droughts can also have legacy effects for years to come and these legacy effects can vary
between the forests according to species and structure (Yu et al., 2022).

Terrestrial biosphere models (TBMs) represent state-of-the-art methods for modelling vegetation fluxes, are versatile tools
35 for studying the effects of climate on biogeochemical cycles, and the only tools for predicting land carbon balance in future
(Blyth et al., 2021). However, TBMs exhibit significant inconsistencies in their simulated results over space and time, re-
sulting from diverging representations of important biogeochemical processes (O'Sullivan et al., 2022). Most TBMs simulate
photosynthesis through the Farquhar-von Caemmerer-Berry (F_cB) kinetic enzyme model (Farquhar et al., 1980), where photo-
synthetic capacity is represented by the maximum carboxylation capacity (normalised to 25 °C; $V_{c(max),25}$) and the maximum
40 rate of electron transport (normalised to 25 °C; $J_{(max),25}$). In recent decades, many TBMs have also incorporated elements of
the N cycle, to varying degrees (Thornton et al., 2009; Sokolov et al., 2008; Zaehle and Friend, 2010). However, this inclu-
sion presents many challenges, particularly in how models represent the N limitation of photosynthesis (Medlyn et al., 2015;
Thomas et al., 2015; Walker et al., 2021). Various modelling approaches to the N cycle have resulted in different ecosystem
responses e.g. to carbon dioxide (CO₂) fertilization (Arora et al., 2020; Meyerholt et al., 2020a; Thomas et al., 2013). As TBMs
45 are crucial for estimating the global terrestrial C sink, it is paramount that the effects of N constraints on plant productivity are
accurately simulated (Zaehle and Dalmonech, 2011).

Given the importance of N in physiological, biochemical and structural processes, novel data sources linked to the N-cycle
and its connections to the C-cycle are highly needed (Kou-Giesbrecht et al., 2023; Meyerholt et al., 2020b). Remotely-sensed
observations of ecosystem traits are an important means of parameterising the temporal dynamics of these models in a spatially-
50 explicit manner (Rogers et al., 2017). Satellite observations have shown that the LAI has increased globally and has contributed
to increase in land carbon sink (Chen et al., 2019) and changing of the Bowen ratio of the energy fluxes (Forzieri et al., 2020).



Simultaneously, lowering of leaf N content has been observed through intensive long-term monitoring plots in European forests (Jonard et al., 2015). One candidate that brings N observations and remote sensing together is leaf chlorophyll content (Chl_{Leaf}), which can be used as a proxy of the photosynthetic N component (Croft et al., 2017) and can be accurately retrieved at ecologically-relevant time and space resolution from remote sensing data, due to the presence of large absorption features in spectral bands typically sampled by optical sensors (Croft and Chen, 2018). There is a large body of literature on leaf chlorophyll retrieval from remote sensing data (Sims and Gamon, 2002; Dash and Curran, 2004), leading to the creation of large-scale national and global products spanning several years (e.g. (Croft et al., 2020)). Integrating physiological information through Chl_{Leaf} data has led to developments to improve modelling gross primary productivity (GPP). For example, Houborg et al. (2013) developed a semi-empirical relationship between Chl_{Leaf} and $V_{c(max),25}$ and used remotely sensed Chl_{Leaf} to replace $V_{c(max),25}$ in the CLM model to improve simulations of gross primary productivity (GPP) for a maize field. Lu et al. (2022) used observations of Chl_{Leaf} and $V_{c(max),25}$ to create plant functional type (PFT)-dependent linear relationships and successfully retrieved the $V_{c(max),25}$ parameter at several ecosystems. At the site level, at the Borden Forest Research Station (hereafter referred to as Borden Forest), Luo et al. (2018) improved GPP modelling by directly linking the seasonal cycle of the $V_{c(max),25}$ parameter to Chl_{Leaf} . Our present study differs from previous literature in that we model Chl_{Leaf} explicitly, and it is based on a predicted nitrogen cycle.

In this research, we use the long time series of in situ LAI and Chl_{Leaf} observations at Borden Forest together with eddy covariance observations of carbon fluxes over a decadal time scale. The long-term nature of the continuous flux record at Borden Forest, with 23 years of near-continuous data provides an almost unparalleled opportunity to examine longer-term trends in ecosystem processes at a deciduous forest site due to warming temperature against a background of temperature and drought variability and extremes and their legacy effects. The seasonal cycle of LAI has several implications to the climate-vegetation exchange, including influencing canopy conductance and fluxes of water, energy and carbon dioxide (Richardson et al., 2013). The development of Chl_{Leaf} and canopy structural parameters, such as leaf area index (LAI) decouple during the shoulder seasons in deciduous forests, necessitating the separate parameterisation of leaf-level physiological processes and LAI in TBMs (Croft et al., 2015). Continuous long-term ground-based observations of LAI at site scale (Rogers et al., 2021) provide a means to assess these phenomenon in one forest.

In our research, the data are combined with a terrestrial biosphere model QUINCY (QUantifying Interactions between terrestrial Nutrient CYcles and the climate system) (Thum et al., 2019), which simulates fully coupled cycles of carbon, nitrogen, phosphorus of terrestrial ecosystems coupled representations of the surface and sub-surface budgets of water and energy. QUINCY is one of the few TBMs that explicitly represents relationships between time-varying foliar nitrogen content, which vary given the ecosystems nutrient availability and carbon-uptake capacity, and the leaf's chlorophyll content (Chl_{Leaf}) and photosynthetic activity (such as $V_{c(max),25}$). The model treats the impact of leaf chlorophyll and its vertical distribution on leaf- and canopy-level photosynthesis using an extension of the FcB model Kull and Kruijt (1998). QUINCY includes a representation of plant growth separating sink and source processes, acclimation of many ecophysiological processes to meteorological and/or nutrient availability and explicit representation of vertical soil processes. Whilst the impacts of climatic events and longer-term climatic shifts are complex to model, we hypothesize that QUINCY can capture changes in ecosystem function



if they are related to meteorological conditions and atmospheric CO_2 . Additionally QUINCY has potential to capture legacy effects of extreme events via its carbohydrate pool structure. This improved modelling capacity will enable to us better understand the nitrogen and carbon cycles under both episodic events, and over inter-annual and decadal timescales in a temperate
90 Deciduous-Boreal ecotone. The diverse observations available at the site allow us to evaluate the model's performance in several aspects. The following four research questions are addressed in this work:

- How does the decoupling of LAI and Chl_{Leaf} seasonal development in the model affect the estimation of annual carbon fluxes?
- Is the QUINCY model able to simulate any long-term changes in seasonal shifts in carbon fluxes and LAI values?
- 95 – Is there a nitrogen constraint on carbon fluxes at Borden Forest, and does it change over the 23-year period?
- Can the QUINCY model simulate the effects of drought events on the carbon cycle?

2 Materials and methods

2.1 Study site

Borden Forest ($44^\circ 19' \text{ N}$, $79^\circ 56' \text{ W}$) is a mixed forest situated in Southern Ontario, Canada. This forest is located in the
100 Great Lakes-St. Lawrence forest ecotone, which is a transition zone that includes both southern temperate forest species and northern boreal species (Froelich et al., 2015). Based on the 2006 vegetation survey (Teklemariam et al., 2009), the forest species composition was primarily composed of red maple (*Acer rubrum*) and eastern white pine (*Pinus strobus*) with 52% and 14% respectively. Other species included large-tooth aspen (*Populus grandidentata*, 8%) white ash (*Fraxinus americana*, 7%), and trembling aspen (*Populus tremuloides*, 3%). The forest has 15-20% evergreen coniferous vegetation. The forest has been
105 naturally regrown from farmland that was abandoned in the early 20th century, with a canopy height of approximately 22 m (Froelich et al., 2015). The soil consists mainly of sand with a thin layer of organic matter. The mean annual temperature at the site is 7.4°C and mean annual precipitation is 784 mm (Froelich et al., 2015). The site is a member of the AmeriFlux network (site-ID: CA-Cbo).

2.2 Site level observations

110 Site-level measurements of carbon fluxes, meteorology and soil moisture, LAI, leaf nitrogen and Chl_{Leaf} and biochemical model parameters ($J_{(max),25}$ and $V_{c(max),25}$) were used in the study. In this study, we define LAI as half of the total (all-sided) leaf area per unit of ground area (Chen and Black, 1992). Three data sets were used, two of which were long-term: i) carbon fluxes, meteorology (1996-2018) and ii) LAI (1998-2018), along with a leaf-level biochemical dataset from 2013 to 2016. Meteorological data was used to force our model simulations, while soil moisture and temperature observations (from years
115 2005-2015) were used to evaluate the model's performance.



2.2.1 Net ecosystem exchange (NEE) of CO₂, meteorological and soil moisture observations

CO₂ flux data from half-hourly eddy covariance measurements sampled at Borden Forest tower at 33 m height between 1996 and 2018 were used. The instrumentation is described in detail in Froelich et al. (2015). No observations were made in 2004 due to instrument and tower replacement. The fluxes were determined on a half-hourly time scale using a program developed at SUNY Albany (Froelich et al., 2015) up to 2013, and using EddyPro (Fratini and Mauder, 2014) thereafter. The vegetation remains uninterrupted from 1.5-4 km towards the southeast and southwest and 1 km towards the northeast. However, there is a cropland less than 400 m in the northwest direction. Data for wind directions between 285° and 20° were excluded from analysis due to insufficient fetch (Luo et al., 2018). Also observations recorded when the friction velocity was less than 0.3 m s⁻¹ were removed according to Froelich et al. (2015), and the data were gap-filled and the measured carbon dioxide net ecosystem exchange (NEE) flux was partitioned into half-hourly gross primary production (GPP) and total ecosystem respiration (TER) according to Barr et al. (2004).

Air temperature, relative humidity, air pressure, longwave and shortwave radiation, wind speed and direction data were also measured from instruments on the flux tower Froelich et al. (2015). For the air temperature, relative humidity, radiation and wind speed we used observations made at 42 metres, for air pressure observations at 2 metres. Soil temperature (from 5 to 100 cm depth) and profiles (depths from 2 to 100 cm) were measured at two locations Froelich et al. (2015), one located 40 m southwest of the flux tower, the other one was located 50 m west. Precipitation data was obtained from the nearby Egbert weather station (44° 23' N, 79° 78' W), which has provided hourly observations since 2014. Prior to 2014, the hourly precipitation was obtained from the ERA5-Land product (Muñoz Sabater et al., 2021) and scaled to match the annual precipitation values as estimated from the hourly Egbert observations. In addition, the ERA5-Land product was used in the gapfilling of observed meteorological data.

2.2.2 LAI observations

We used a daily LAI time series of 1999-2018 from Rogers et al. (2021), estimated from photosynthetically active radiation (PAR) observations collected above and below the canopy. PAR was measured above the canopy by LI-COR LI-190SA (LI-COR, Lincoln Nebraska) sensor and below the canopy with a LI-COR LI-191 sensor. We estimated daily LAI values from half-hourly observations of above-canopy and transmitted PAR using the Miller integral (Miller, 1967), as recommended by Rogers et al. (2021). To improve spatial representativeness of the daily LAI estimates at the site, the values were then calibrated to match effective LAI (L_e) measured along a 100m transect using a handheld LI-COR LAI-2000 plant canopy analyzer (LI-COR, Lincoln Nebraska) using a linear relationship. True LAI was estimated from all the observations as:

$$LAI = \frac{[(1 - \alpha)L_e\gamma_E]}{\Omega_E} \quad (1)$$

where α is the ratio of woody area to total area and γ_E is the ratio of needle area to shoot area (taken as unity in deciduous forests). The value of α (0.17) was taken from the literature (Gower et al., 1999), similar to Croft et al. (2015). The clumping



index (Ω_E) is 0.95, was measured using a TRAC (Tracing Radiation and Architecture of Canopies) instrument (Huiming Instrumentation Limited, Nanjing, China) Rogers et al. (2021).

2.2.3 Leaf-level trait measurements

150 In situ leaf-level data included measurements of Chl_{Leaf} and nitrogen content, maximum electron transport and carboxylation capacities ($J_{max,25}$, $V_{c(max),25}$), and specific leaf area (SLA). The measurements were collected at an average interval of 9 days during the growing seasons (day of year 130-290) from 2013 to 2016. In 2013, only leaf chlorophyll and SLA data were collected. In 2014, all six variables were measured. In the following years, only chlorophyll, $J_{max,25}$ and $V_{c(max),25}$ were measured. For these biochemical measurements, leaves were sampled from the top of the canopy from the flux tower. Leaf-
155 level gas exchange measurements were made using a LI-6400 portable infrared gas analyzer (LI-COR, Lincoln, Nebraska, USA) (Croft et al., 2017). Chl_{Leaf} and leaf nitrogen content were destructively analyzed in the laboratory from five sampled leaves per measurement date. The methodology and the measurements are described in detail in Croft et al. (2013, 2014); Wellburn (1994). The SLA was calculated as the ratio of leaf area to leaf dry mass. In this study, we used a species-weighted canopy average of the leaf-level parameters, based on the species composition of the forest (i.e. red maple 60.4 %, large-tooth
160 aspen 12.9 %, trembling aspen 12.4 % and ash 14.2 %) Croft et al. (2015).

2.3 The QUINCY model

2.3.1 General description

The QUINCY model (QUantifying Interactions between terrestrial Nutrient CYcles and the climate system) (Thum et al., 2019) was used to simulate ecosystem functioning in the study area. QUINCY simulates fully coupled carbon, nitrogen and
165 phosphorus cycles as well as water and energy balances in vegetation and soil on a half-hourly time scale. Here we give a brief description of the model, focusing on the parts relevant to this study. A more detailed description can be found in Thum et al. (2019).

Vegetation is grouped by Plant Functional Type (PFT), and represented as an average individual composed of structural pools (leaves, sapwood, heartwood, coarse roots, fine roots and fruits), a labile pool (a fast overturning and respiring non-structural
170 pool) and a reserve pool (seasonal, non-respiring and non-structural storage pool). The non-structural pools represent storage pools for non-structural carbohydrates and associated nutrients. Trees are also characterized by height (m), diameter (m) and stand density (m^{-2}). The tree canopy is composed of ten canopy layers, which increase in depth (of LAI) exponentially with layer depth (LAI_{cl}). Photosynthesis and stomatal conductance are calculated separately for the sunlit and shaded leaves in each layer, as estimated by a radiative transfer model (see below) (Zaehle and Friend, 2010) using a Farquhar model based
175 scheme from Kull and Kruijt (1998). According to this scheme, the role of leaf chlorophyll is explicitly taken into account in the photosynthesis calculation and determines the proportion of the leaf area at each canopy layer that is light-saturated. The photosynthesis for the non-light-saturated part is calculated using the light-limited rate of photosynthesis (relying on the $J_{max,25}$ parameter). The photosynthesis in the light-saturated part is calculated as a co-limited rate of the electron transport



capacity (determined using $J_{max,25}$) and carboxylation capacity (via Rubisco; determined using $V_{c(max,25)}$). Therefore both
180 biochemical model parameters and leaf chlorophyll influence photosynthesis. Determination of these rates from leaf nitrogen
is described in Section 2.3.3. The leaf stoichiometry can be set fixed or it can be dynamic, when it is varied in response to
nutrient demand and supply.

Stomatal conductance is modelled after Medlyn et al. (2011) and in addition to stomatal conductance, soil moisture can limit
photosynthesis directly through a modifier in calculation of the biochemical parameters (Egea et al., 2011). Photosynthesis can
185 also be down-regulated by the sink limitation (example in Fig. S1 in Thum et al. (2019)).

Maintenance respiration is a linear function of the N content of each pool. Temperature acclimation for photosynthesis is as
in Friend (2010) and for maintenance respiration as in Atkin et al. (2014). Tissue growth is defined by allometric equations, and
the allometric relationship between leaves and fine roots responds to N and water limitation by increasing the uptake capacity
under nutrient limitation.

190 Soil biogeochemistry is largely based on a CENTURY-style (Parton et al., 1993) approach, except that the vertical soil
profile of biogeochemical pools, including metabolic, structural and woody litter as well as fast and slow overturning soil
organic matter (SOM), is explicitly represented. Each soil layer also includes N pools of ammonium (NH_4) and nitrate (NO_3).
The soil profile consists of 15 layers, reaching a depth of 9.5 metres. The depth of each layer increases exponentially as it
goes deeper. The stoichiometry of the litter is determined by the stoichiometry of the plant pool it comes from. The fast pool's
195 stoichiometry is dependent on the availability of inorganic nutrients, while the slow pool has a fixed stoichiometry. Plants and
microbes compete for the nutrients based on their respective demand and uptake capacity. NH_4 is oxidized to NO_3 through
nitrification in the aerobic part of the soil and NO_3 is reduced to diatomic nitrogen N_2 through denitrification in the anaerobic
part of the soil (Zaehle et al., 2011). Both processes also produce nitrogen oxide NO_y and nitrous oxide N_2O . Biological
nitrogen fixation (BNF) is considered as an asymbiotic and symbiotic process (Meyerholt et al., 2016).

200 Soil temperature and moisture are calculated for each layer based on soil physical characteristics, as well as the transport
and atmospheric exchange of energy and water. The radiative transfer scheme has been developed following the two-stream
approach by Spitters (1986) and the original implementation to OCN (Zaehle and Friend, 2010) has been extended to include
diagnostic canopy albedo, clumping and attenuation of the shortwave backscatter from the soil. The radiative transfer is cal-
culated separately for the visible and near-infrared radiation bands. It estimates the sunlit and shaded leaves for each canopy
205 layer and separates the incoming radiation into direct and diffuse components.

2.3.2 Phenology of the deciduous trees

The seasonal development of leaf biomass is affected by the plant's ability to grow new tissues and the fractional allocation
to plant organs. The start and end of the growing season are determined by meteorological and soil moisture values, which
are averaged over seven days to mitigate the impact of daily climate variability. The start of the growing season is determined
210 by the accumulated growing degree days (GDD_{acc} , which represents the current number of growing degree days above the
temperature threshold, t_{air}^{GDD} , since the beginning of last dormancy period) as:



$$GDD_{acc} > GDD_{req}^{max} \times \exp^{-k_{dormancy}^{GDD} \times NDD}, \text{ where} \quad (2a)$$

$$\frac{GDD_{acc}}{dt} = GDD_{acc} + \text{MAX}(t_{air} - t_{air}^{GDD}, 0.0) \quad (2b)$$

NDD is the number of dormancy days, taken as days since the last growing season, and $k_{dormancy}^{GDD}$ (value 0.007 days^{-1}) relates dormancy to the maximum growing degree-day requirement (GDD_{req}^{max} , 800 degree-days) to account for the chilling requirements of the buds (Krunner et al., 2005), and dt denotes the time step in days. The growing season ends when the decreasing average air temperature falls below the temperature threshold of (t_{air}^{sen} , $8.5 \text{ }^\circ\text{C}$) and then senescence occurs.

2.3.3 Leaf N partitioning

While the overall amount of leaf nitrogen is largely driven by phenological development, the leaf N concentration per leaf area (N_{leaf}) responds to soil nutrient availability, as plants take up mineral N from the soil pools. This uptake is determined by the amount of N in each soil pool and fine root biomass, and is further modulated by plant N demand. Leaf nitrogen has a vertical gradient that decreases exponentially towards the bottom of the canopy, in accordance with observations (Niinemets et al., 1998). Leaf N in each layer ($N_{leaf,cl}$) is divided into structural and photosynthetic parts (Friend et al., 1997). The fraction of structural N ($fN_{struc,cl}$) is calculated for each canopy layer as a function of the total leaf N in the respective layer (Zaehle and Friend, 2010):

$$fN_{struc,cl} = k_0^{struc} - k_1^{struc} N_{leaf,cl} \quad (3)$$

k_0^{struc} is the maximum fraction of structural leaf N (0.63 for deciduous forest (Friend et al., 1997; Kattge et al., 2011)) and k_1^{struc} is an the slope of structural leaf N with total N ($7.14 \times 10^3 \text{ g}^{-1}\text{N}$) (Friend et al., 1997) .

The photosynthetic N pools have three compartments: Rubisco associated (fN_{rub}), electron transport associated (fN_{et}), and chlorophyll associated (fN_{chl}). The photosynthetic fractions all have a role in the calculation of photosynthesis (Kull and Kruijt, 1998). The fractions are used directly in the calculation of the photosynthetic parameters $V_{c(max),25}$ and $J_{max,25}$, where the leaf N in each content is multiplied with these fractions and some other modifiers (equations S7 and S10 in Thum et al. (2019)). According to Zaehle and Friend (2010), the fraction of leaf N in chlorophyll is calculated to increase with canopy depth:

$$fN_{chl} = \frac{k_0^{chl} - k_1^{chl} e^{-k_{fn}^{chl} LAI_c}}{a_{chl}^n}, \quad (4)$$

where k_0^{chl} (value 6.0 (Zaehle and Friend, 2010)), k_1^{chl} (value 3.6 (Zaehle and Friend, 2010)) and k_{fn}^{chl} (value 0.7 (Friend, 2001)) are empirical parameters. a_{chl}^n is the molecular N content of chlorophyll ($25.12 \frac{\text{mol}}{\text{mmol}^{-1}}$ (Evans, 1989)). LAI_c is the cumulative leaf area.



The photosynthetic parameters $V_{c(max),25}$ and $J_{max,25}$ are assumed to have a fixed ratio of 1.97 (Wullschleger, 1993). Based
240 on this ratio, fN_{rub} and fN_{et} are calculated, using the calculated values of the structural and chlorophyll fractions.

2.3.4 Modelling protocol

The QUINCY model requires half-hourly meteorological forcing, including short and longwave radiation, air temperature,
precipitation, air pressure, humidity, wind speed as well as atmospheric CO_2 concentration (hereafter referred to as $[CO_2]$),
and N and P deposition rates. Meteorological forcing was measured at the site and the $[CO_2]$ was obtained from Friedlingstein
245 et al. (2019) and N deposition data from Lamarque et al. (2010, 2011). The Borden forest is described as a broadleaf deciduous
forest PFT and we performed point scale simulations.

To obtain a near-equilibrium state of soil and vegetation, the model was spun up for 500 years, using atmospheric CO_2
concentration from a randomly selected year from the 1901-1930 period and a random year of observed meteorological data.
This was followed by a transient simulation starting in 1901. This used the atmospheric $[CO_2]$ and N deposition values derived
250 from data sources mentioned above and, from 1996 onwards, the measured site-level meteorology for the respective years. For
the purposes of this study, we ran simulations where only the C or both the C and N cycles were active. In the simulation where
only C was active, the plants had access to all the N that they needed. The P concentration was kept at a level, where it did not
limit plant uptake or SOM decomposition. The temperature response of the BNF (Bytnerowicz et al., 2022) was set to have an
optimum temperature of 18 °C, replacing the default value of 32 °C. The default value is based on observations in the tropics
255 and the shape of the curve predicts very low BNF for more northern regions with the default optimum temperature. Lowering
this value to typical air temperature at the Borden site provides more realistic BNF for the site and assumes local temperature
acclimation. The SLA is a constant value of 320 $cm\ g^{-1}$ for the broadleaf deciduous forest PFT in the model simulations. To
compare to the leaf level observations (Chl_{Leaf} , $V_{c(max),25}$, $J_{max,25}$) made at the top of the canopy, we used only the top
canopy layer values from the model.

260 The model was run with several different parametrizations to study the influence of using LAI and Chl_{Leaf} on the param-
eterisation and how their decoupling influences the results. For the carbon cycle-only (C-only) simulation, we show results
from the original model formulation (orig), then with the simulation using LAI to tune phenology (LAI tuning, C-only:LAI)
and finally a simulation using both LAI and Chl_{Leaf} for tuning (C-only:LAI&chl). These simulations have been done with
dynamic leaf stoichiometry, that is basically showing forest at N saturation. This simulation is showed in the first sections of
265 this paper, since the nitrogen cycle enabled version showed too low GPP at the site and we also wanted to show the influence
of model tuning with LAI and Chl_{Leaf} with GPP levels comparable to the observations. For comprehensiveness, we also
report the values for the carbon cycle-only simulations with fixed stoichiometry, which reflects the C cycle with average N
availability, but with no N limitation on growth and soil processes.

For the C-only and CN simulation, we use the results after both LAI and Chl_{Leaf} in the main analysis. The abbreviations of
270 the model simulations are found in Table 1. A schematic figure (Fig. S1) showing the work flow of the study, with the parameter
tuning and then comparison to the observations in found in the SI.



t

Table 1. Abbreviations used for the model runs.

Abbreviation	Explanation
C-only:orig	C cycle only enabled model simulation with original parameters, with dynamic leaf stoichiometry
C-only:LAI	C cycle only enabled model simulation with parameter tuning based on LAI, with dynamic leaf stoichiometry
C-only:LAI&chl	On top of C-only:LAI simulation also parameter tuning based on Chl_{Leaf} , with dynamic leaf stoichiometry
C-only,fix:orig	C cycle only enabled model simulation with original parameters, with fixed leaf stoichiometry
C-only,fix:LAI	C cycle only enabled model simulation with parameter tuning based on LAI, with fixed leaf stoichiometry
C-only,fix:LAI&chl	On top of C-only:LAI simulation also parameter tuning based on Chl_{Leaf} , with fixed leaf stoichiometry
CN:orig	Simulation including N cycle with original parameters
CN:LAI	Simulation including N cycle with parameter tuning based on LAI
CN:LAI&chl	On top of CN:LAI simulation also parameter tuning based on Chl_{Leaf}

The original parameter values and the tuned parameter values are shown in Table 2. We adjusted the parameters by comparing the modelled LAI and Chl_{Leaf} to the observations (Fig. 1b, c) and tried to match those. To adjust the seasonality of LAI, the parameter controlling leaf senescence (t_{air}^{sen}) was modified from the default value of 8.5 °C to 15.0 °C. It is likely that leaf senescence at the site is partially controlled by light availability, a process which is not yet present in the model, therefore the higher temperature threshold is accounting for this missing factor. To adjust the summertime magnitude of Chl_{Leaf} parameters k_0^{struc} (Eq. 3) and k_0^{chl} (Eq. 4) were adjusted. In the model the whole leaf nitrogen is initially allocated to the structural nitrogen during the initial stages of the growing season. Subsequently, the amount allocated to the photosynthetic compartments (including leaf chlorophyll, $V_{c(max),25}$ and $J_{max,25}$) begins to increase as the season progresses. The model was modified to incorporate a delay in the transition from structural nitrogen to photosynthetic nitrogen. We added in a delay of 20 days by introducing a leaf age factor to the simulations (equations for this change: Eqs. S1-S3) in the C-only simulations and delay of fifteen days in the CN CN,fix -simulations.

2.3.5 Estimation of seasonal metrics and trends

We estimated the growing season metrics separately using GPP or LAI. The start and end of the season (SOS and EOS) estimated from GPP were calculated from the first and last pass of the threshold, which was defined as the 30 % of the year's 90th percentile value (an example year of 2014 in Fig. S2a). For the LAI the threshold was calculated as being the 20 % of the difference between the summer and winter values, starting from the winter value (Fig. S2b). Length of the growing season (LOS) is the time between SOS and EOS. These calculations were made on smoothed data using an averaging weekly window to minimise anomalies. The trend assessment was carried out with a particular focus on statistically significant trends, which were identified through the application of Student's t-test on slope values obtained from the linear regression ($p < 0.05$).



t

Table 2. Parameter values in different simulations. The unit of the parameter in parenthesis after the parameter name.

Simulation	t_{air}^{sen} (°C)	k_0^{struc} (-)	k_0^{chl} (-)
C-only:orig	8.5	0.63	6.0
C-only:LAI	15.0	0.63	6.0
C-only:LAI&chl	15.0	0.68	5.2
C-only,fix:orig	8.5	0.63	6.0
C-only,fix:LAI	15.0	0.63	6.0
C-only,fix:LAI&chl	15.0	0.50	7.0
CN:orig	8.5	0.63	6.0
CN:LAI	15.0	0.63	6.0
CN:LAI&chl	15.0	0.58	6.5

3 Results

3.1 Dynamic parameterisation of LAI and leaf chlorophyll content improves modelled GPP estimates

The average modelled GPP, LAI and leaf Chl_{Leaf} values for the three C-only C cycle model simulations (C-only:orig, C-only:LAI and C-only:LAI&chl) across a growing season from 1996-2018 are shown alongside the measured data in Fig. 1 a, c, e. The observed GPP starts to increase already after day of year (DOY) 100, whereas in all the simulations, the increase begins later and at a faster rate. The increase to maximum summer time values in the simulations happens rapidly and the maximum summer values occur early in the season, around DOY 160 (early June). The observations show more shallow decrease, with maximum summertime values occurring around DOY 200 (mid-July).

At the end of the season, the inclusion of LAI (C-only:LAI) and Chl_{Leaf} (C-only:LAI&chl) data improved the representation of senescence at the end of the season, and the consequent decline in GPP, compared to the C-only:orig simulation. The summertime average was accurately simulated by the model, with an average overestimation of 1.1 % for June, July and August with the C-only:orig and C-only:LAI simulations and 5.0 % overestimation with the C-only:LAI&chl simulation (Fig. 1a). The annual carbon flux values together with root mean square error (RMSE) and R-squared (r^2) are shown in Table S1 and scatterplots with daily observed GPP values and simulated GPP from different parameterizations is in Fig. S3. The different C-only model simulations did not largely impact RMSE and r^2 values.

The simulations with the N constraint on carbon fluxes (CN simulation) demonstrate a reduction in summertime GPP values, with the averaged GPP during July-August underestimated by 14 % compared to observations (Fig. 1 b). The same modification to the phenology parameter was made as in the C-only simulation, with the objective of improving the fit of the simulated LAI (simulation CN:LAI). This resulted in a more accurate representation of the observed seasonal cycles of GPP, LAI and Chl_{Leaf} in the simulations (Fig. 1 b, d, f).

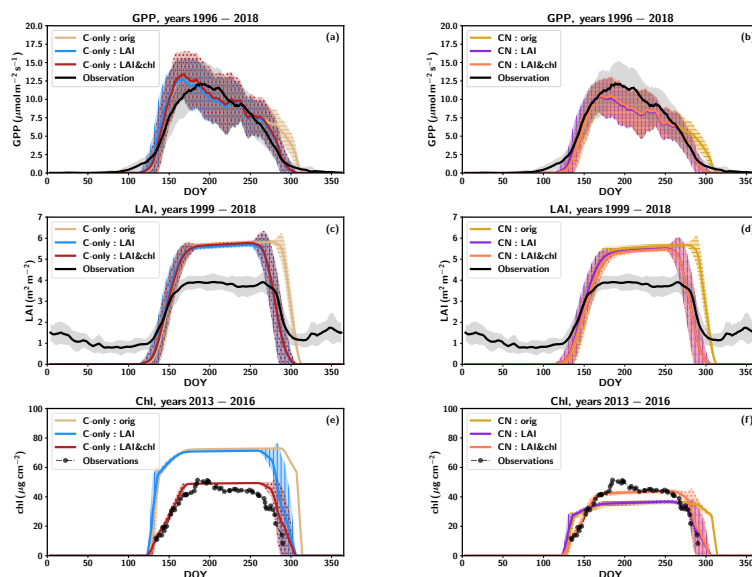


Figure 1. Averaged yearly cycles of a) gross primary production (GPP), c) leaf area index (LAI) and e) leaf chlorophyll from the C-only simulations and for the CN-simulations GPP in b), LAI in d) and leaf chlorophyll in f). The shaded regions show the standard deviations between the years. The observations are represented by a black line, while the QUINCY results with the original model C-only formulation are shown in light brown, with LAI tuning (C-only:LAI) in blue, and with the LAI and leaf chlorophyll tuning (C-only:LAI&chl) in red. The CN:orig simulation results are in dark yellow and CN:LAI results in magenta and the CN:LAI&chl in orange. In (a) and (b), the data represents the mean values for the period 1996-2018. In (c) and (d), the data represents the mean values for the period 1999-2018 and in (e) and (f) for the period 2013-2016. The lines have been smoothed with a seven-day averaging window, except for the observed leaf chlorophyll has been smoothed with a three-day window.

The use of the LAI in the model tuning had a more pronounced impact on the GPP fluxes in both the C-only and CN simulations because of shortening the growing season, even though the changes in r^2 (order of 0.01) or RMSE remain relatively minor. After the LAI and Chl_{Leaf} tuning, the simulation had a 3.6 % overestimation in the annual GPP in the C-only simulations and an underestimation by 17 % in the CN simulations (Table S1). The impact of the N constraint on the annual GPP was $302 \text{ gC m}^{-2} \text{ yr}^{-1}$ (Table S1), representing a 20 % decrease in the annual GPP value relative to the C-only simulation. When considering the C-only,fix:LAI&chl simulation, the estimated GPP was very similar to the CN-simulations, with on 1.4 % larger value (Table S1).

From this point onward in the paper, when we refer to the C-only simulations, we refer to the results from the simulations with the LAI and Chl_{Leaf} tuning (C-only:LAI&chl), and similarly for CN simulations. CN:LAI&chl was the most successful of the simulations in terms of r^2 and RMSE when compared against observed GPP (Table S2).



3.2 Other carbon fluxes: TER and NEE

The total ecosystem respiration (TER) was decreased compared to the original simulation after altering the parameters (Table 2) for both C-only and CN-simulations (Table S1). This is connected to the declining GPP, as the litter input influences the amount of soil carbon. The CN simulations had better r^2 values for TER than the C-only simulations (Table S1). This occurred
325 because the magnitude of TER was better captured by these simulations (Fig. S4). The most pronounced underestimation of the TER in the CN simulations by the model compared to the observations occurs during the summer months July and August (Fig. S4, 2b).

The observed annual TER was overestimated by the C-only simulation by 18 % (Table S1). The CN-simulation yielded a more accurate representation of the annual estimate, which was 6 % lower than the observed value (Table S1). The C-
330 only,fix:LAI&chl simulation gave similar values to the CN-simulation, with 1.2 % larger annual value (Table 1). The nitrogen cycle was found to constrain annual TER by $300 \text{ gC m}^{-2} \text{ yr}^{-1}$, representing a 20 % decrease from the C-only simulation.

The observations indicated that the forest acted as a sink, with a net carbon uptake of $-205 \pm 140 \text{ gC m}^{-2} \text{ yr}^{-1}$ over the measurement period. The simulations indicated that it was a weak sink, for both the C-only and the CN simulations, with very small difference (Table S1). However, it should be noted that the interannual variation in the simulations was considerable.
335 During the summertime the sink of the ecosystem was underestimated in the C-only simulations (Fig. S5). Despite the GPP summertime magnitude being underestimated in the CN-simulations, the performance of the model as estimated by the r^2 and RMSE, was for NEE and the component fluxes better with the CN than C-only simulations (r^2 better by 0.08 for GPP, 0.12 for TER, 0.15 for NEE) (Table S1, Fig. S6).

The early season pattern observed in the simulated NEE is attributed to heterotrophic respiration (Fig. 2a and b, S7), which
340 is regulated by the soil moisture and soil temperature in the model. QUINCY is simulating these soil conditions based on the meteorological conditions and soil texture. The majority of the simulated heterotrophic respiration originates from the uppermost soil layers. Consequently, the soil temperature of the upmost layer is represented (Fig. 2c). The soil temperature is significantly underestimated during the winter months, and increase to the summertime levels occurs earlier in the simulations than in the observations. This phenomenon occurs during the period between day of year (DOY) 70 and 150. It is during this
345 time that the TER is being overestimated in the spring (Fig 2b, c). The maintenance respiration is also activated during this time period, although its increase is less pronounced due to the temperature acclimation (Fig. S7). In autumn, the simulated drawdown of the TER occurs simultaneously with the observations, despite the simulated soil temperature decreasing at a faster rate than that observed (Fig. 2).

The soil conditions are relevant for estimation of the TER, as heterotrophic respiration is an important part of it (Fig. S7).
350 The too early increase of simulated soil temperatures in spring occurs also at deeper depths (Fig. S8). Also at deeper levels at 10 and 20 cm the wintertime soil moisture is underestimated. The observed summertime variability of soil moisture is better captured by the model in deeper layers than in the 5 cm depth, even though the summertime magnitude is overestimated at 10 cm depth (Fig. S8).

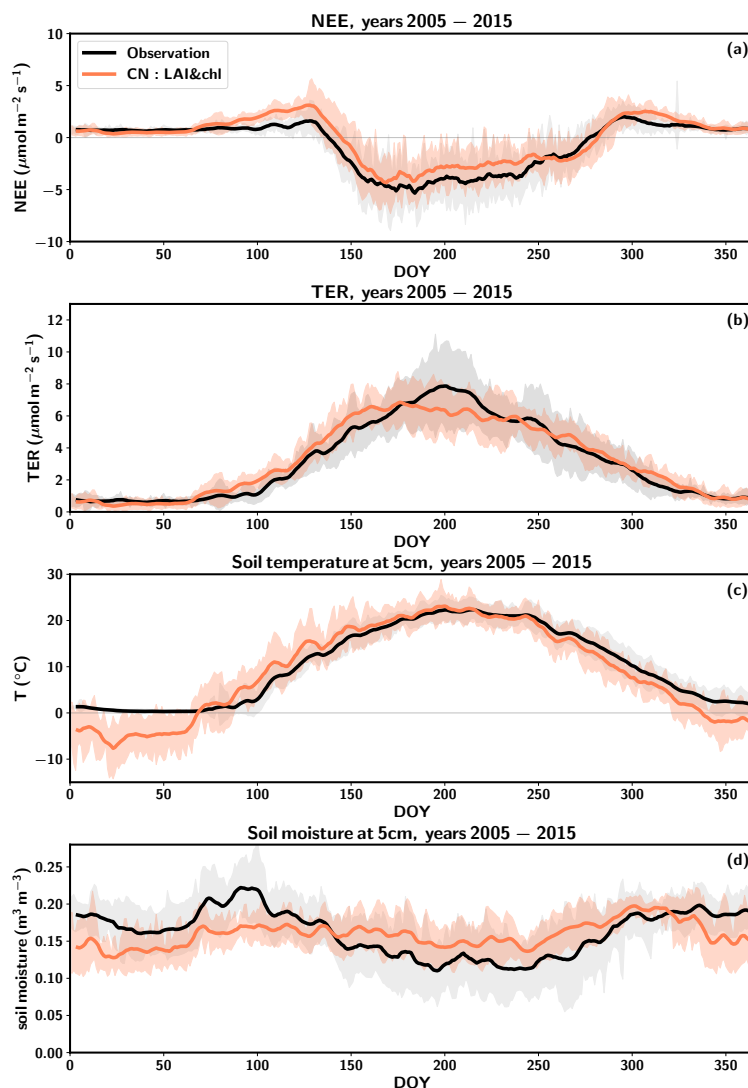


Figure 2. Averaged seasonal cycles of net ecosystem exchange, NEE (a), total ecosystem respiration, TER (b), soil temperature at 5 cm depth (c) and soil moisture (d) averaged over the period 2005-2015. The observations are represented in black, the CN:LAI&chl model results in orange and the standard deviation is shown by the shaded regions. Both the observations and simulations are smoothed with a seven-day window.

3.3 Simulated structural and biochemical parameters

355 The continuous observations of LAI provide values ($3.78 \pm 0.43 \text{ m}^2 \text{ m}^{-2}$ in summer, averaged the over June-July period, along with the standard deviation). The simulated values were closer to the LAI-2000 observations than to the values obtained from the continuous observations. The LAI-2000 observations have a summertime average of $4.63 \pm 0.71 \text{ m}^2 \text{ m}^{-2}$ for years 2013-



t

Table 3. Observed and simulated (C-only:LAI&chl and CN:LAI&chl simulations) leaf traits. Values are estimated for the June-July means with standard deviations. The unit of the parameter in parenthesis after the parameter name. For the LAI the values 1998-2018, for leaf N and the biochemical parameters 2014 and for Chl_{Leaf} 2013-2016.

Variable (unit)	Observed	Simulation (C-only:LAI&chl)	Simulation (CN:LAI&chl)
LAI (continuous) ($m^2 m^{-2}$)	3.78 ± 0.43	5.27 ± 0.77	4.77 ± 0.91
Leaf N (gm^{-2})	1.32 ± 0.13	4.21 ± 0.13	2.10 ± 0.09
$J_{max,25}$ ($\mu mol m^{-2} s^{-1}$)	117.1 ± 24.2	296.6 ± 53.5	164.7 ± 27.1
$V_{c(max),25}$ ($\mu mol m^{-2} s^{-1}$)	63.5 ± 14.4	156.8 ± 28.2	87.1 ± 14.2
Chl_{Leaf} ($\mu g cm^{-2}$)	45.6 ± 7.9	45.9 ± 6.1	40.8 ± 4.0

2018. The C-only simulation overestimated continuous observations by 39 %, while the overestimation in CN simulations was 26 % (Table 3). The LAI from the CN simulations was closer to the value estimated from the LAI-2000 observations, with
360 only 3 % overestimation.

The C-only simulation (C-only:LAI&chl) overestimated observed leaf N by approximately threefold (Table 3). The CN-simulation (CN:LAI&chl) overestimated the observed value by 59 %. The photosynthetic parameters in the model are derived directly from the leaf N concentration. For the C-only simulation, this resulted in a pronounced overestimation of the photosynthetic parameters. The C-only simulation (C-only:LAI&chl) estimated a 2.5-fold overestimation of observed $J_{max,25}$ (Fig. 3a,
365 Table 3). The estimated value for $J_{max,25}$ derived from the CN-simulations (CN:LAI&chl) was higher than the the observed value by 41 % (Fig. 3, Table 3). The C-only simulation (C-only:LAI&chl) overestimated the observed $V_{c(max),25}$ 2.4-fold, while the CN simulation (CN:LAI) overestimated it by 37 % (Fig. 3, Table 3). These high predicted value are not unexpected, given the direct link between plant N and photosynthetic parameters in the model and the implicit unlimited N availability in the C-only model.

370 The tuning of the model did not have a pronounced effect on the summertime magnitude of the photosynthetic parameters (Fig. 3), because the changes in the nitrogen allocated to leaf chlorophyll were derived from the structural nitrogen. However, the tuning did influence the fraction of photosynthetic part of nitrogen and therefore a small decrease in photosynthetic parameters was noticed in C-only tuning, when level of Chl_{Leaf} was decreased and a small increase occurred in CN tuning, when the level of Chl_{Leaf} was increased (Fig. 3). The springtime delay imposed on the leaf chlorophyll also influenced the
375 photosynthesis parameters, resulting in an improved seasonal cycle compared to observations (Figs. 3).

The specific leaf area (SLA) exhibited a dynamic change in the observations, with higher values ($303 cm g^{-1}$) observed in the early season and a subsequent decline to a summertime value of $162 cm g^{-1}$ within approximately one month.

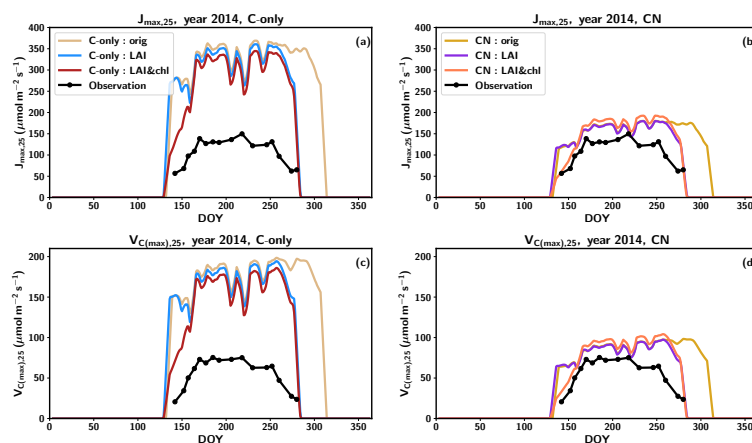


Figure 3. The seasonal cycle of $J_{max,25}$ (a, c) and $V_{C(max),25}$ (b, c) in 2014 with C-only simulations (a, c) and CN simulations (b, d). The observations are represented in black, the original QUINCY results from the C-only simulations in light brown, with LAI tuning in blue and with both LAI and leaf chlorophyll tuning in violet. The CN:orig simulation results are in dark yellow, the CN:LAI in magenta and CN:LAI&chl in orange. The modelling results have been averaged with a seven-day smoothing window.

3.4 The influence of drought on carbon fluxes

A severe drought occurred at the site in 2007, when the precipitation was approximately 20 % lower than in a regular year, at 608 mm yr⁻¹ (Fig. S9). Fig. 4 depicts the averages over the time period 2005-2015 (with the exception of 2007 and 2008) for GPP, TER and soil moisture at 5 cm, as the soil moisture observations were available for this time period. The annual observed TER in 2007 was clearly below the average annual TER by 37 % (i.e. 794 gC m⁻²yr⁻¹) and the level remained low throughout the summer. The following year 2008 was characterized by higher-than average precipitation (923 mm yr⁻¹), 21 % above average; Fig. S9). Furthermore, the summertime maximum TER values in 2008 were below average (Fig. 4c). Additionally, the values of TER exhibited a slower rate of increase and a more rapid decrease to winter levels after mid-summer compared to regular years (Fig. 4c). This resulted in the observed TER for 2008 being 36 % below the averaged annual TER (i.e. 804 gC m⁻²yr⁻¹). In contrast to the measurements, the simulations did not predict low TER for the beginning of the season in 2007 or 2008. Instead, the behaviour in the CN simulations was similar to that observed in other years (Fig. 4d). Only, when there was a pronounced decrease in soil moisture around DOY 160 in 2007, decrease in the simulated TER resulted. Following the precipitation event around DOY 200, the TER values exhibited a recovery to typical summertime levels for several days. After this a decline to lower levels occurred. The precipitation events that occurred around DOY 240 resulted in TER returning to a regular level. The simulated GPP also exhibited a regular pattern in both years until DOY 160 (Fig. 4b). In 2007 the decline and recovery followed a similar pattern to TER.

Observed GPP exhibited a decline in 2007, with the annual value being 24 % lower (i.e. 1112 gC m⁻²yr⁻¹) compared to the averaged annual GPP. In 2008, the observed GPP was found to be lower than in 2007, with a value of 1086 gC m⁻²yr⁻¹, representing a 26% decline below the average. A later increase of GPP to summer values in spring and an earlier decrease to

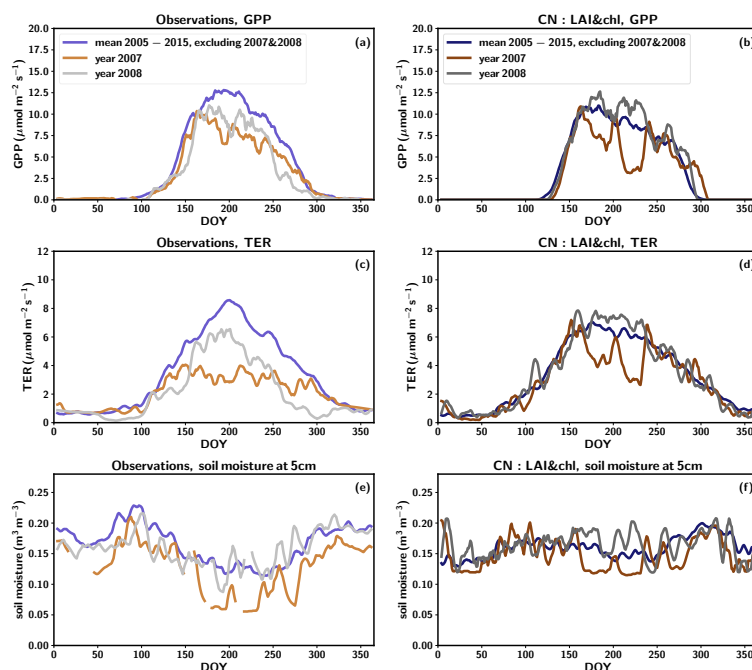


Figure 4. The averaged seasonal cycles for observations and CN-simulations for gross primary production, GPP (a and b), total ecosystem respiration, TER (c and d) and soil moisture at 5 cm (e and f). The averaged seasonal cycle for 2005-2015 without 2007 and 2008 is in violet, year 2007 in brown and year 2008 in grey. The simulation results are in darker shade than the observations. Both the observations and the model results have been smoothed using a seven-day averaging window.

winter values were responsible for the reduction in the annual value, with peak season GPP being higher than in 2007 (Fig. 4a). The measured soil moisture was consistently below the typical values throughout 2007 and that continued until early summer of 2008 (DOY 150, Fig. 4e.) The annual simulated GPP (CN:LAI&chl simulations) was 14 % lower and the annual simulated
400 TER was 9 % lower in 2007 compared to regular years. In 2007 the simulated soil moisture was generally at a higher level compared to observations, but showed rather similar responses to precipitation events than observations (Fig. 4e, f). Overall, the simulated soil moisture exhibits a narrower range than the observed soil moisture data in regular years, and declines less in the drought year than observations. In 2008 the simulated carbon fluxes were found to be 15 % higher than the averaged annual means for GPP and 10 % higher for TER (Fig. 4b, d).

405 The model demonstrated a less pronounced effect of drought on the carbon fluxes than was observed in 2007. Furthermore, the likely legacy effects of drought that were observed in 2008 were not replicated by the model. In regular years a hysteresis effect of TER versus the soil temperature relationship was observed, with the values in the later half of the year having lower values (Fig. S10a). In drought year 2007 this effect was not visible, with values staying at a low level. In 2008 the hysteresis effect was more pronounced than in 2006. The model simulations were not able to replicate this kind of behaviour. The
410 observed soil moisture at 5 cm depth did not explain the observed hysteresis effect (data not shown). As a possible explanation



t

Table 4. The average start of season (SOS), end of season (EOS) and length of season (LOS) as determined from the observations and the QUINCY model simulation (CN:LAI&chl) of GPP and LAI.

Variable	unit	Observations	QUINCY
SOS (GPP)	DOY	137	139
SOS (LAI)	DOY	139	140
EOS (GPP)	DOY	281	285
EOS (LAI)	DOY	294	287
LOS (GPP)	days	144	143
LOS (LAI)	days	155	147

to the hysteresis effect, one could think about strong connection between the photosynthesis and respiration. The observations indeed show a higher GPP in early summer months compared to later months in the year, especially in 2008 (Fig. S11). This phenomenon does not take place in the simulations (Fig. S11b, d, f).

3.5 Interannual variability and longer term trends in annual carbon fluxes

415 The growing season metrics were estimated based on both LAI and GPP from the observations and CN:LAI&chl simulation. The start of season (SOS) takes place almost at the same time according to the GPP and LAI based estimates, the end of season (EOS) is estimated to be some days later in LAI bases estimates (Table 4). The simulations agree on both observation-based estimates of SOS by couple of days, and there is a larger difference between the observed and simulated EOS estimates. The simulated EOS based on LAI is earlier than observed (Table 4). In the simulations the GPP and LAI are tightly coupled.
420 However, in the observations the EOS estimated from LAI takes place in average 13 days later than the EOS according to the GPP. The observed LAI remains high, despite decreasing GPP. LAI is therefore not so tightly coupled to the seasonality of GPP in autumn as it is in the model. C-only simulations provide similar estimates for these growing season metrics.

The time series of the metrics indicates that the EOS from simulations has a larger range of variability (38 days from GPP estimated EOS) than the observations (27 days from GPP estimated, 18 days from LAI estimated) (Fig. 5b). Additionally,
425 the simulations demonstrated a greater interannual variation in the SOS estimation (range 34 days for LAI-based estimation) than seen in the observations (range 20 days for GPP-based estimation, 32 days for LAI-based estimation) (Fig. 5a). Stronger interannual variability in model estimates of LAI is driven by the phenological parameters governed by air temperature. The real forest with several species might have more resilience to different environmental conditions and therefore be able to make use of different spring and autumn periods. No discernible trends are evident in any of the time series under consideration. The
430 cold spring of 2018 resulted in the simulation estimates of SOS occurring at a later point in time, although the impact was not as pronounced in the observations of GPP (Fig. 5).

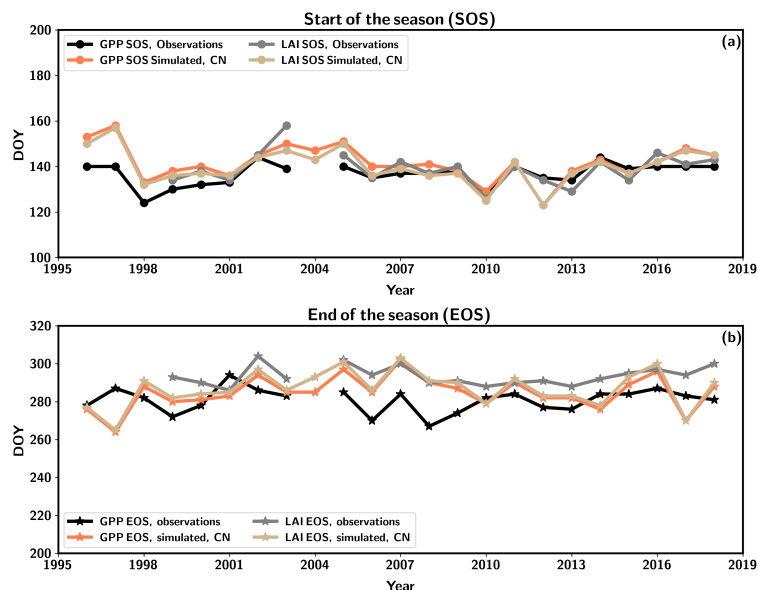


Figure 5. The start of season (SOS) (a) and end of season (EOS) (b) as estimated from observed and simulated (CN:LAI&chl) time series of GPP (black observation, orange simulation) and LAI (gray observation, light brown simulation).

The next step involved the calculation of trends for the annual values of GPP, TER and NEE (Fig. S12, Table S2) derived from the CN:LAI&chl simulations. In order to assess the ability of QUINCY to capture observed interannual fluctuations in the annual carbon balance, the changes were investigated over time. This was done with a particular focus on statistically significant trends, which were identified through the application of Student's t-test ($p < 0.05$). During the time period 1996-2018 the observed GPP exhibited a significant increasing trend (Fig. S12, Table S2), with a magnitude of $22.4 \text{ gC m}^2 \text{ yr}^{-1} \text{ yr}^{-1}$. A significant trend was also present in the summertime and autumn observations (Table S2). QUINCY showed a minor and non-significant upward trend for GPP (Table S2). When the final five years of the data series were excluded, the observed GPP trend was no longer statistically significant and had decreased to $11.6 \text{ gC m}^2 \text{ yr}^{-1} \text{ yr}^{-1}$. This was comparable to the QUINCY estimation for the same period, which was $8.6 \text{ gC m}^2 \text{ yr}^{-1} \text{ yr}^{-1}$.

The observed TER in the period from 1996 to 2018 showed a non-significant trend of $9.0 \text{ gC m}^2 \text{ yr}^{-1} \text{ yr}^{-1}$, which was a bit larger than the significant trend seen in TER from QUINCY, $6.9 \text{ gC m}^2 \text{ yr}^{-1} \text{ yr}^{-1}$. The observations indicated a significant trend for NEE towards a larger sink, with a rate of $-13.4 \text{ gC m}^2 \text{ yr}^{-1} \text{ yr}^{-1}$ over the same time period. The simulations instead proposed an increasing source, with a magnitude of $5.2 \text{ gC m}^2 \text{ yr}^{-1} \text{ yr}^{-1}$. The continuous observations of summertime LAI (averaged over June, July and August) showed a significant trend of $0.033 \text{ m}^2 \text{ m}^{-2} \text{ yr}^{-1}$. The QUINCY model estimated a minor non-significant negative trend ($-0.001 \text{ m}^2 \text{ m}^{-2} \text{ yr}^{-1}$). Tuning done for the LAI and Chl_{Leaf} did not influence the simulated trends.

The GPP estimates derived from the CN simulation found to be in close agreement with the observations until 2010 (Fig. S12a). However, a divergence is observed between the simulations and observations from that point onwards. The observations



450 indicate an increase, whereas the simulations remain at a consistent level before declining in the last three years ((Fig. S12a). In the observations the interannual variation is found to be more pronounced in TER than GPP. In contrast, the simulations indicate that the interannual variation is greater in the GPP than TER.

4 Discussion

In this study we employed a variety of observational data sources in conjunction with a terrestrial biosphere model. Our
455 objective was to assess the utility of these data in enhancing and evaluating the model's performance, as well as to ascertain the model's capacity to simulate the biogeochemical cycles within the Borden forest. Our focus extends beyond the carbon cycle, as our modelling approach incorporates the nitrogen cycle, for which the available observational data provides valuable insights.

4.1 Using the continuous LAI observations

460 The site-level continuous LAI observations provide a valuable data source for model evaluation and development. Our simulations showed a discrepancy between the absolute value of LAI and these observations. Despite QUINCY underestimating the summertime GPP by approximately 14% in the CN:LAI&chl simulations, the simulated LAI was overestimated (Fig. 1 d). The LAI estimated from litterfall at the site was $5.1 \text{ m}^2 \text{ m}^{-2}$ (Neumann et al., 1989) and in close agreement with the model estimate of $5.3 \text{ m}^2 \text{ m}^{-2}$ derived from the C-only simulations and $4.8 \text{ m}^2 \text{ m}^{-2}$ derived from the CN-simulations.

465 Tuning of the senescence parameter (Table 2) resulted in substantially higher temperature threshold for the start of the senescence period at the site compared to the standard parameterisation. As described in Section 2.3.2, the phenology model of QUINCY is a simple growing-degree based formulation and does not take into account other environmental conditions such as light availability or day-length, which might be contributing to early leaf senescence. Day-length in particular has been shown to be another important variable controlling senescence in these regions Bowling et al. (2024). Future work will
470 address whether implementing such a dependency in QUINCY improves the seasonality of LAI estimation without adjusting the temperature threshold for senescence.

The continuous measurements are of particular value for assessing model seasonality, as they provide continuous data, unlike the point values obtained from LAI-2000 or litterfall. Therefore, using these data to improve the seasonality of the modelled LAI is a logical approach. By adjusting the senescence in accordance with the LAI observations, it is possible to improve the
475 seasonal cycle of GPP, as the senescence was occurring too late in the default model at this site (Fig. 1). In this context, the continuous measurement of LAI is of particular significance, as it represents an independent measure from the carbon fluxes that can also be observed from space.

4.2 Other leaf-level observations

In addition to LAI, there were several other leaf-level observations at the site, which we used in our model evaluation. In
480 the original QUINCY formulation the development of leaf chlorophyll is fully coupled to the LAI development (Thum et al.,



2019). However, observations reveal a clear decoupling taking place during the early season (Croft et al., 2017). The approach we have adopted here is to delay the development of leaf chlorophyll from the structural, i.e. non-photosynthetic, nitrogen. Previous studies at the site indicated that leaf chlorophyll lags 30 days behind LAI in reaching its maximum summertime value (Croft et al., 2015). However, the difference observed in the modelling was less pronounced, as the objective was to accurately represent the seasonal development of leaf chlorophyll correctly, while the observed maximum value of Chl_{Leaf} was reached 485 later than the simulated summertime maximum level (Figs. 1c). The observed Chl_{Leaf} values exhibit elevated levels during the midsummer period, spanning approximately one month. In the modelling conducted, the objective was not to replicate this specific behaviour but rather to capture the average summertime level.

Another variable that undergoes changes during the spring season in the observations is the specific leaf area (SLA). Rather than delaying the onset of chlorophyll development from the structural nitrogen, it would be possible to introduce a dynamically 490 changing SLA to QUINCY, as the leaves are thinner immediately following budburst. The SLA in QUINCY is set to a PFT-specific, time-invariant constant representative of the average observed value in (Kattge et al., 2011), which is almost double the observed summertime value at Borden forest. This overestimation may contribute to the large LAI predicted for the site by QUINCY, as the SLA is used in the leaf area calculation (Thum et al., 2019). Testing dynamically changing SLA in the model 495 falls outside the scope of our current study, but is an important future step for improving predictions of leaf process seasonality.

4.3 Limitations of the model

It should be noted that, like with any other modelling study, our modelling approach is subject to certain limitations, due to the necessity of making certain simplifications. Borden forest is a mixed forest, and the different deciduous species differ in their leaf chlorophyll contents and SLA values (Croft et al., 2017), and likely their responses to climate variability. Our 500 modelling approach does not allow for species separation; instead, we are estimating the tree traits per average individual for a deciduous forest. The rationale behind our approach can be attributed to the large scale that we are aiming to model and the focus on utilisation of parameters that can be derived from remote sensing observations which are unavailable at a scale where individual trees (and their species) can be resolved.

Another challenge in characterising the forest as a deciduous PFT is the exclusion of the coniferous trees at the site. This leads 505 to discrepancies in our wintertime estimates of LAI, as the simulated deciduous trees lack leaves during this season. Another effect can be seen in the delay of the simulated GPP increase in the spring, which occurs in the observations after DOY 100 (Fig. 1a, b). This is partly due to the understorey vegetation, which we do not simulate, and partly due to the coniferous trees at the site, which can start photosynthesis as soon as meteorological conditions and the release of possible winter acclimation allow. The shape of the seasonal cycle of GPP is also different in the simulations compared to the observations (Fig. 1 b). 510 The increase in the simulations is more abrupt to the summer levels and decline from early summer values occurs quite early, probably due to drought occurrences. This could be due to the fact that the observed transitions is more smooth in time as several tree species contribute to the trend, which is represented only by one functional type in the model. Issues with species mixtures are common in TBMs and while this is certainly an area that needs further improvement it is not an issue unique to the model used here.



515 Testing model performance a TBM designed for large-scale simulation at site-level is challenging as the model necessarily
needs to apply generalizations in process representation in order to have a model that can be applied across sites and at
large scales, due to limited knowledge and data needed for large-scale parameterization. Of particular importance to this
study is the parameterisation of the partitioning of nitrogen into different compartments, which has a theoretical basis (Evans,
1989), however, the approach applied in QUINCY is simple and relies on PFT-specific parameterization, with very limited
520 consideration of leaf-level data. The dataset available for the Borden site is very valuable in this respect, as it allows evaluating
the division of nitrogen to different compartments. The parameterization used in QUINCY does not take all factors into account.
For example, the phosphorus content has been shown to influence the relationship between the $V_{c(max),25}$ and leaf nitrogen
(Walker et al., 2014). Furthermore, the description of the canopy nitrogen gradient in QUINCY appears to be sound, but it may
not account for all possible variation (Niinemets et al., 2015). Borden forest is located in the temperate boreal forest ecotone
525 and many species are close to the limits of their temperature and moisture ranges (Froelich et al., 2015). The tree species
composition has undergone changes at the site during our study period, e.g. the red maple was reported to have coverage of
36 % in 1995 (Lee et al., 1999) and 52 % in 2006 (Teklemariam et al., 2009). The impacts that these changes in the tree
composition have on the carbon fluxes could be studied by a demographic model with sufficient granularity in the description
of tree functional diversity (see Fisher et al. (2018) for a review).

530 4.4 Legacy effects of drought

Carbon fluxes at the site were strongly influenced by the 2007 drought, which also led to legacy effects visible in 2008 (Fig. 4).
Often the effect of drought on GPP is stronger than on TER (Schwalm et al., 2010; Piao et al., 2019b), but here a stronger effect
on TER was observed. GPP can be reduced by drought through both physiological and structural effects (van der Molen et al.,
2011). No decrease in the LAI was observed at the site in 2007 or 2008. One of the recognised mechanisms for legacy effects
535 is that the drought-induced decrease in GPP can lead to a decrease in the carbohydrate pool and therefore influence the LAI
development in the following year (Yu et al., 2022). QUINCY has an explicit reserve pool and could theoretically simulate
this type of behaviour, but did not suggest that such legacy effects affected the GPP in 2008. Although the simulated soil
moisture shows a similar dynamic behaviour to the observations (Fig. 4), simulated top-soil moisture did not show the same
dynamic range of moisture seasonal cycle magnitude and minimum in QUINCY when compared to the in-situ observations,
540 possibly explaining underestimated response to soil moisture stress by the model. However, we note the modelled range was
more similar to the observations at deeper depths than the top layer (Fig. S8e, f). At present, it is unclear whether this reflects
shortcomings in the representation of soil physical processes or is a result of the lack of in-situ precipitation observations during
the study period (See Methods).

There are many possible explanations for the strong legacy effect observed in TER in 2008. Soil microbial activity is
545 dependent on soil moisture (Gaumont-Guay et al., 2006; Liu et al., 2009; Orchard and Cook, 1983) and drought can thus
strongly reduce soil respiration directly and indirectly through several different mechanisms (von Buttlar et al., 2018). Direct
effects include the dependence on the presence of water films for substrate diffusion and exo-enzyme activity (Davidson and
Janssens, 2006) as well as microbial dormancy and death (Orchard and Cook, 1983). Indirect effects affect microbial activity



through, for example, changes in soil nutrient retention and availability (Bloor and Bardgett, 2012) or changes in microbial
550 community structure (Frank et al., 2015). In addition, GPP and TER fluxes are tightly coupled, as heterotrophic respiration is
also driven by the recently assimilated carbon and not only by environmental conditions (Ruehr et al., 2012). QUINCY was
not able to capture the drought-induced decrease in TER in 2007, which could either be due to a too low impact of the drought
on soil moisture, or the fact that the version of QUINCY applied here does not simulate microbial activity and root exudation
(Yu et al., 2020). This also contributes to the failure to simulate potential legacy effects in the observed TER (Fig. 4).

555 The drought response at the site could potentially be improved by calibrating the soil moisture response functions in the
model, but probably some structural changes in the description of soil physics, such as water-retention curve, would also
be required. Soil moisture is a challenge for many models and often in need of improvement (De Pue et al., 2023). Future
research will investigate whether a more sophisticated soil biogeochemical model can better represent the effects on microbial
communities and through them the legacy effects on respiration (Yu et al., 2020). Overall, terrestrial biosphere models are not
560 yet well equipped to capture the legacy effects (Bastos et al., 2021) and more work is needed to better understand the processes
governing ecosystem recovery in order to improve models in this respect.

4.5 Seasonality in the total ecosystem respiration

QUINCY is generally capable of modelling the observed magnitude and seasonal amplitude of observed TER, based on em-
pirical responses of soil organic turnover to soil temperature and moisture (Table S2). The premature increase in the simulated
565 soil respiration occurs during average years due to a too early increase in the soil temperature in the simulations (Fig. 2). This
behaviour suggests that the coupling between the atmosphere and the soil in the model is too strong, which may be associated
with parameters controlling heat diffusion in the soil.

One interesting feature observed in the TER is the strong seasonality in respect to soil temperature in normal years, which
cannot be explained by the soil moisture (Fig. S10). This behaviour was first discussed by Lee et al. (1999) at this site and they
570 called it the hysteresis effect. It occurs most pronounced in the year following the drought, 2008 (Fig. S10e). Based on the data
available then, Lee et al. (1999) found the early season had lower respiration values than the late season and speculated that
this difference might be due to warmer soil temperatures in deeper soil layers as the season progressed, as well as greater litter
accumulation. The data available to-date for a longer period shows an "inverse" hysteresis effect, in which the later season has
lower TER than the early season (Fig. S10a and e). Soil moisture does not provide an explanation for such a shift. Rather, this
575 behaviour could be driven by the seasonality of photosynthesis, as the early season GPP co-incides with lower soil temperatures
compared to the late season (Fig. S11). A fast coupling between GPP and soil respiration, e.g through photosynthesis supplying
carbohydrates to rhizosphere respiration (Zhang et al., 2018), could explain the observed hysteresis effect. Hysteresis effects
on soil respiration versus soil temperature are quite common (Zhang et al., 2018), and further explanations for dynamics taking
place at Borden could be caused by substrate depletion late in summer (Kirschbaum, 2006) or by greater root productivity in
580 early season (Oe et al., 2011). Models generally describe soil respiration as a function of soil temperature responses and would
not capture the hysteresis effects (Zhang et al., 2018). This is also the case for QUINCY, which is not able to capture this



hysteresis effect (Fig. S11). Future work should evaluate whether including for instance increased vegetation-soil coupling via root exudates, would improve the representation of the interannual variability of TER.

4.6 Trends and growing season length

585 There were no significant changes in the growing season metrics SOS, EOS and LOS over the period studied, similar to Gonsamo et al. (2015). QUINCY was generally successful in simulating these metrics, but the end of season as estimated from GPP and LAI differed in the observations, whereas it was coupled in the model. The previous studies at the site that have assessed the growing season metrics (Froelich et al., 2015; Gonsamo et al., 2015) also used the carbon uptake period (CUP). We did not assess CUP because its onset would have been biased in the simulations due to the premature increase in
590 heterotrophic respiration caused by the premature increase in soil temperature (Fig. 2).

Froelich et al. (2015) found a significant increase in summertime GPP and Gonsamo et al. (2015) significant increase in carbon uptake. These are consistent with our observational results, which additionally also showed a small but significant increase in the summertime LAI. The increase in net carbon uptake is attributed to increased PAR (photosynthetically active radiation, 400-700 nm), which leads to increased photosynthetic activity (Gonsamo et al., 2015). There have been reductions in
595 atmospheric sulfur, nitrogen oxides, total nitrates and ozone since 1992 and the brightening has been attributed to reductions in gaseous and particulate emissions, while declines in ozone emissions reduce the damages to the leaves (Gonsamo et al., 2015).

The observed trend in PAR is not detectable in the shortwave downward radiation flux used as input by the model. As the model assumes a constant ratio of shortwave downward radiation to PAR, QUINCY does simulate then an effect of increased PAR on photosynthesis. One additional cause of model failure might be that the canopy light-saturation point does not reflect
600 the observations, however, there is not robust evidence that this is the case. Furthermore, the QUINCY model does not take into account potential damage to the leaves caused by ozone. Ozone influences both photosynthesis and stomatal conductance and can cause them to become decoupled (Novak et al., 2005; Lombardozzi et al., 2015). Estimates of decreases in the photosynthesis by 21 % and in stomatal conductance by 11% after chronic ozone exposure have been estimated (Lombardozzi et al., 2013), but also lower estimates have been presented (6-10% for Europe) (Franz et al., 2017). Ozone exposure can also have
605 impact on the N cycle (Simpson et al., 2014). The impact of ozone has been modelled by direct influence on $V_{c(max),25}$ and stomatal conductance (Lombardozzi et al., 2012) or then on photosynthesis, which then has feedbacks on stomatal conductance (Franz et al., 2017; Lombardozzi et al., 2015).

QUINCY approximately reproduces the leaf-level photosynthetic parameters in the CN version of the model, but at the same time overestimates LAI (compared to the continuous observations) and underestimates GPP. The uncertainty in the annual flux
610 estimates by the eddy covariance method is usually around 10-20 % (Loescher et al., 2006), so QUINCY's estimates are within the uncertainty of the observations. Possible reasons for this discrepancy are the lack of understorey representation in the model, the simplified representation of the mixed forest with a single deciduous plant functional type, and possible biases introduced by the assumed within-canopy gradient of leaf nitrogen, which might not hold for this diverse forest. It is interesting to note that the differences between the annual GPP and carbon balance are not apparent in the early years of the record, but
615 emerge in the later years (Fig. S12). The underestimation of annual GPP is 13 % by the CN:LAI&chl simulations for the whole



period, but only 8 % for the years 1996-2010. Therefore, the increasing trend in observed GPP that the model fails to reproduce is contributing strongly to the model-data discrepancy.

4.7 Impact of nitrogen cycle on the carbon fluxes

Including the nitrogen cycle in the simulations did not cause a change the net carbon balance of the ecosystem, as both the GPP and TER were both attenuated by approximately the same amount, about 20 % when comparing to the C-only version with N saturation. With the fixed stoichiometry the C-only model gave similar values to the CN simulations (Table S1). This denotes that there was not nitrogen constraint on the carbon fluxes according to the QUINCY model. The leaf C:N was only 9.7 in the C-only:LAI&chl saturated case simulation, which is unrealistically low value, but we chose to show these results here to assess the influence of parameterization with simulations with magnitudes comparable to the observed GPP. The foliar C:N ratio was 20.4 in the CN:LAI&chl simulation and 22.4 in the C-only,fix:LAI&chl, showing that they are similar.

Nitrogen availability limits the carbon cycle (Du et al., 2020), especially in the boreal region (Högberg et al., 2017). The estimated effect of the N cycle on the carbon fluxes is not as large as some previous estimates (Thornton et al., 2007). The summertime variation in GPP values is more pronounced in the C-only simulations with dynamic stoichiometry than in the CN simulations (Fig. S3a), highlighting the more stable behaviour of the model when including the N constraint and compared to N saturated case. Although the annual GPP was underestimated with the inclusion of the N cycle, after tuning by both LAI and Chl_{Leaf} , the CN simulation gave best r^2 and RMSE metrics for both GPP and TER, and in line with the C-cycle simulations with fixed stoichiometry (Table S1).

4.8 Using of site level observations in model development

The different site level observations available at the site provided means to evaluate the model performance from different aspects. The QUINCY model is a large scale model and cannot capture all the small scale variations. Furthermore, the different tree species in Borden complicate simulating the forest with QUINCY, as the model needs to rely on a general PFT description. However, to better understand the processes occurring at the site some further observations would be useful. To capture the forest structure and to facilitate estimation of the radiative transfer inside the canopy, LiDAR observations (Balestra et al., 2024) would be beneficial, and if done on temporally continuous scale (such as in StrucNet, see Calders et al. (2023)), also valuable information on allocation of annual net primary production could be obtained. Soil chamber observations of respiration would help to separate the role of soil in the total ecosystem respiration. Use of isotopes would enable revealing the processes behind the observed hysteresis behaviour of the soil respiration. Rain gauge at the site would help to study potential biases of using precipitation data at a nearby site. The ozone profile concentration observation at the site could help in estimating the potential ozone damages on the vegetation, that could be addressed by a model.



645 5 Conclusions

In this work we used several data streams measured at the Borden Forest Research Station, some extending over two decades, and aimed to improve and evaluate the terrestrial biosphere model QUINCY. This work demonstrated the usefulness of using different data sources and the importance of long time spans. The use of leaf chlorophyll content and LAI improved simulated GPP in the CN simulations. These changes also decreased the RMSE for TER. Generally the model did capture average
650 seasonal cycle of GPP (daily $r^2=0.80$) and TER (daily $r^2=0.75$). QUINCY was also successful in estimation of the growing season metrics, even though the ending of the season was more coupled between LAI and GPP than in the observations.

The evaluation of the soil physical states and soil carbon fluxes revealed a need for model improvement. The soil temperature data showed that QUINCY is biased towards too early an increase in soil temperature in spring, which directly affects the simulated heterotrophic respiration. The simulated soil moisture did not capture the full range of observed variability in topmost
655 layer, which could lead to too weak a drought response of the simulated carbon fluxes. The drought experienced at the site in 2007 had a pronounced effect on carbon fluxes, which was also prevalent in the following year. QUINCY was not able to reproduce this behaviour. The noticeable trend seen in the observed annual GPP values was not captured by the model, but since it has been attributed to the increase in PAR and not visible in the shortwave radiation that is used as a meteorological forcing for QUINCY, this is not surprising.

660 Two important data sources used in this work, leaf chlorophyll content and leaf area index (LAI), can also be measured from space. Therefore our work paves the way toward combining terrestrial biosphere models (TBMs) and using remote sensing data for their parameterization, as has been proposed by Rogers et al. (2017). Work in this front has been done by combining leaf chlorophyll to the photosynthesis parameters of models (Lu et al., 2022). In this work we explicitly model the leaf chlorophyll, which links this variable directly to the nitrogen cycle. The unique dataset accessible from the Borden site permitted the
665 assessment and enhancement of the parameterization employed to divide leaf nitrogen to different compartments. In addition to utilising LAI and leaf chlorophyll, sun-induced chlorophyll fluorescence (SIF) represents a pivotal variable observed from space that is linked to the carbon cycle (Sun et al., 2023). SIF is currently being implemented in QUINCY and will, in the future, provide a means of conducting a global-scale assessments of the carbon cycle together with the nitrogen cycle related metrics.

670 *Data availability.* Data, including model results from the CN:LAI&chl simulations and meteorological forcing used to run the model, can be found at [10.57707/fmi-b2share.81778e9da06243d5bccdd364cfdb320a](https://doi.org/10.57707/fmi-b2share.81778e9da06243d5bccdd364cfdb320a).

Author contributions. TT designed the study. OS did preliminary analysis and code modifications proposed by SZ. TM performed final analysis and made the figures. HC, RS and CR provided observation data. TT wrote the first version of the manuscript. The interpretation of the results was developed in discussions with all the authors. The manuscript was commented by all the authors.



675 *Competing interests.* The authors declare no competing interests.

Acknowledgements. We acknowledge the CA-Cbo AmeriFlux site for its data records. In addition, funding for AmeriFlux data resources was provided by the U.S. Department of Energy's Office of Science. TT, TM and OS acknowledge funding from Research Council of Finland (RESEMON project, grant number 330165; and 337552), and for TM, also Flagship of Advanced Mathematics for Sensing Imaging and Modelling, grant number 359196). Scientific programmers Dr. Jan Engel and Dr. Julia Nabel are thanked for technical support and
680 maintenance of the QUINCY code. Dr. Manon Sabot is thanked for useful discussions.



References

- Arora, V. K., Katavouta, A., Williams, R. G., Jones, C. D., Brovkin, V., Friedlingstein, P., Schwinger, J., Bopp, L., Boucher, O., Cadule, P., Chamberlain, M. A., Christian, J. R., Delire, C., Fisher, R. A., Hajima, T., Ilyina, T., Joetzjer, E., Kawamiya, M., Koven, C. D., Krasting, J. P., Law, R. M., Lawrence, D. M., Lenton, A., Lindsay, K., Pongratz, J., Raddatz, T., Séférian, R., Tachiiri, K., Tjiputra, J. F., Wiltshire, A., Wu, T., and Ziehn, T.: Carbon–concentration and carbon–climate feedbacks in CMIP6 models and their comparison to CMIP5 models, *Biogeosciences*, 17, 4173–4222, <https://doi.org/10.5194/bg-17-4173-2020>, 2020.
- Atkin, O. K., Meir, P., and Turnbull, M. H.: Improving representation of leaf respiration in large-scale predictive climate–vegetation models, *New Phytologist*, 202, 743–748, <https://doi.org/https://doi.org/10.1111/nph.12686>, 2014.
- Balestra, M., Marselis, S., Sankey, T. T., Cabo, C., Liang, X., Mokroš, M., Peng, X., Singh, A., Stereńczak, K., Vega, C., Vincent, G., and Hollaus, M.: LiDAR Data Fusion to Improve Forest Attribute Estimates: A Review, *Current Forestry Reports*, 10, 281–297, <https://doi.org/10.1007/s40725-024-00223-7>, 2024.
- Barr, A. G., Black, T., Hogg, E., Kljun, N., Morgenstern, K., and Nesic, Z.: Inter-annual variability in the leaf area index of a boreal aspen-hazelnut forest in relation to net ecosystem production, *Agricultural and Forest Meteorology*, 126, 237–255, <https://doi.org/https://doi.org/10.1016/j.agrformet.2004.06.011>, 2004.
- Bastos, A., Orth, R., Reichstein, M., Ciais, P., Viovy, N., Zaehle, S., Anthoni, P., Arneth, A., Gentine, P., Joetzjer, E., Lienert, S., Loughran, T., McGuire, P. C., O, S., Pongratz, J., and Sitch, S.: Vulnerability of European ecosystems to two compound dry and hot summers in 2018 and 2019, *Earth System Dynamics*, 12, 1015–1035, <https://doi.org/10.5194/esd-12-1015-2021>, 2021.
- Bloor, J. M. and Bardgett, R. D.: Stability of above-ground and below-ground processes to extreme drought in model grassland ecosystems: Interactions with plant species diversity and soil nitrogen availability, *Perspectives in Plant Ecology, Evolution and Systematics*, 14, 193–204, <https://doi.org/https://doi.org/10.1016/j.ppees.2011.12.001>, 2012.
- Blyth, E. M., Arora, V. K., Clark, D. B., Dadson, S. J., De Kauwe, M. G., Lawrence, D. M., Melton, J. R., Pongratz, J., Turton, R. H., Yoshimura, K., et al.: Advances in land surface modelling, *Current Climate Change Reports*, 7, 45–71, 2021.
- Bowling, D. R., Schädel, C., Smith, K. R., Richardson, A. D., Bahn, M., Arain, M. A., Varlagin, A., Ouimette, A. P., Frank, J. M., Barr, A. G., Mammarella, I., Šigut, L., Foord, V., Burns, S. P., Montagnani, L., Litvak, M. E., Munger, J. W., Ikawa, H., Hollinger, D. Y., Blanken, P. D., Ueyama, M., Matteucci, G., Bernhofer, C., Bohrer, G., Iwata, H., Ibrom, A., Pilegaard, K., Spittlehouse, D. L., Kobayashi, H., Desai, A. R., Staebler, R. M., and Black, T. A.: Phenology of Photosynthesis in Winter-Dormant Temperate and Boreal Forests: Long-Term Observations From Flux Towers and Quantitative Evaluation of Phenology Models, *Journal of Geophysical Research: Biogeosciences*, 129, e2023JG007839, <https://doi.org/https://doi.org/10.1029/2023JG007839>, e2023JG007839 2023JG007839, 2024.
- Bytnerowicz, T. A., Akana, P. R., Griffin, K. L., and Menge, D. N. L.: Temperature sensitivity of woody nitrogen fixation across species and growing temperatures, *Nature Plants*, 8, 209–216, <https://doi.org/10.1038/s41477-021-01090-x>, 2022.
- Calders, K., Brede, B., Newnham, G., Culvenor, D., Armston, J., Bartholomeus, H., Griebel, A., Hayward, J., Junttila, S., Lau, A., Levick, S., Morrone, R., Origo, N., Pfeifer, M., Verbesselt, J., and Herold, M.: StrucNet: a global network for automated vegetation structure monitoring, *Remote Sensing in Ecology and Conservation*, 9, 587–598, <https://doi.org/https://doi.org/10.1002/rse2.333>, 2023.
- Canadell, J., Monteiro, P., Costa, M., Cotrim da Cunha, L., Cox, P., Eliseev, A., Henson, S., Ishii, M., Jaccard, S., Koven, C., Lohila, A., Patra, P., Piao, S., Rogelj, J., Syampungani, S., Zaehle, S., and Zickfeld, K.: Global Carbon and other Biogeochemical Cycles and Feedbacks, in: *Climate Change 2021: The Physical Science Basis. Contribution of Working Group I to the Sixth Assessment Report of the Intergovernmental Panel on Climate Change*, edited by Masson-Delmotte, V., Zhai, P., Pirani, A., Connors, S., Péan, C., Berger, S., Caud,



- N., Chen, Y., Goldfarb, L., Gomis, M., Huang, M., Leitzell, K., Lonnoy, E., Matthews, J., Maycock, T., Waterfield, T., Yelekçi, O., Yu, R., and Zhou, B., Cambridge University Press, Cambridge, UK and New York, NY, USA, <https://doi.org/10.1017/9781009157896.007>, 2022.
- 720 Chen, J. M. and Black, T. A.: Defining leaf area index for non-flat leaves, *Plant, Cell & Environment*, 15, 421–429, <https://doi.org/https://doi.org/10.1111/j.1365-3040.1992.tb00992.x>, 1992.
- Chen, J. M., Ju, W., Ciais, P., Viovy, N., Liu, R., Liu, Y., and Lu, X.: Vegetation structural change since 1981 significantly enhanced the terrestrial carbon sink, *Nature Communications*, 10, 4259, <https://doi.org/10.1038/s41467-019-12257-8>, 2019.
- Croft, H. and Chen, J.: 3.09 - Leaf Pigment Content, in: *Comprehensive Remote Sensing*, edited by Liang, S., pp. 117–142, Elsevier, Oxford, 725 <https://doi.org/https://doi.org/10.1016/B978-0-12-409548-9.10547-0>, 2018.
- Croft, H., Chen, J., Zhang, Y., and Simic, A.: Modelling leaf chlorophyll content in broadleaf and needle leaf canopies from ground, CASI, Landsat TM 5 and MERIS reflectance data, *Remote Sensing of Environment*, 133, 128–140, <https://doi.org/https://doi.org/10.1016/j.rse.2013.02.006>, 2013.
- Croft, H., Chen, J., and Noland, T.: Stand age effects on Boreal forest physiology using a long time-series of satellite data, *Forest Ecology and Management*, 328, 202–208, <https://doi.org/https://doi.org/10.1016/j.foreco.2014.05.023>, 2014.
- 730 Croft, H., Chen, J., Froelich, N., Chen, B., and Staebler, R.: Seasonal controls of canopy chlorophyll content on forest carbon uptake: Implications for GPP modeling, *Journal of Geophysical Research: Biogeosciences*, 120, 1576–1586, 2015.
- Croft, H., Chen, J. M., Luo, X., Bartlett, P., Chen, B., and Staebler, R. M.: Leaf chlorophyll content as a proxy for leaf photosynthetic capacity, *Global change biology*, 23, 3513–3524, 2017.
- 735 Croft, H., Chen, J., Wang, R., Mo, G., Luo, S., Luo, X., He, L., Gonsamo, A., Arabian, J., Zhang, Y., et al.: The global distribution of leaf chlorophyll content, *Remote Sensing of Environment*, 236, 111 479, 2020.
- Dash, J. and Curran, P. J.: The MERIS terrestrial chlorophyll index, *International Journal of Remote Sensing*, 25, 5403–5413, <https://doi.org/10.1080/0143116042000274015>, 2004.
- Davidson, E. A. and Janssens, I. A.: Temperature sensitivity of soil carbon decomposition and feedbacks to climate change, *Nature*, 440, 740 165–173, <https://doi.org/10.1038/nature04514>, 2006.
- De Pue, J., Wieneke, S., Bastos, A., Barrios, J. M., Liu, L., Ciais, P., Arboleda, A., Hamdi, R., Maleki, M., Maignan, F., Gellens-Meulenberghs, F., Janssens, I., and Balzarolo, M.: Temporal variability of observed and simulated gross primary productivity, modulated by vegetation state and hydrometeorological drivers, *Biogeosciences*, 20, 4795–4818, <https://doi.org/10.5194/bg-20-4795-2023>, 2023.
- Du, E., Terrer, C., Pellegrini, A. F. A., Ahlström, A., Van Lissa, C. J., Zhao, X., Xia, N., Wu, X., and Jackson, R. B.: Global patterns of 745 terrestrial nitrogen and phosphorus limitation, *Nature Geoscience*, 13, 221–226, <https://doi.org/10.1038/s41561-019-0530-4>, 2020.
- Egea, G., Verhoef, A., and Vidale, P. L.: Towards an improved and more flexible representation of water stress in coupled photosynthesis–stomatal conductance models, *Agricultural and Forest Meteorology*, 151, 1370–1384, <https://doi.org/https://doi.org/10.1016/j.agrformet.2011.05.019>, 2011.
- Evans, J. R.: Photosynthesis and nitrogen relationships in leaves of C3 plants, *Oecologia*, 78, 9–19, 1989.
- 750 Farquhar, G. D., Von Caemmerer, S., and Berry, J. A.: A biochemical model of photosynthetic CO₂ assimilation in leaves of C3 species, *Planta*, 149, 78–90, <https://doi.org/10.1007/BF00386231>, 1980.
- Fisher, R. A., Koven, C. D., Anderegg, W. R. L., Christoffersen, B. O., Dietze, M. C., Farrior, C. E., Holm, J. A., Hurtt, G. C., Knox, R. G., Lawrence, P. J., Lichstein, J. W., Longo, M., Matheny, A. M., Medvigy, D., Muller-Landau, H. C., Powell, T. L., Serbin, S. P., Sato, H., Shuman, J. K., Smith, B., Trugman, A. T., Viskari, T., Verbeeck, H., Weng, E., Xu, C., Xu, X., Zhang, T., and Moorcroft,



- 755 P. R.: Vegetation demographics in Earth System Models: A review of progress and priorities, *Global Change Biology*, 24, 35–54, <https://doi.org/https://doi.org/10.1111/gcb.13910>, 2018.
- Forzieri, G., Miralles, D. G., Ciais, P., Alkama, R., Ryu, Y., Duveiller, G., Zhang, K., Robertson, E., Kautz, M., Martens, B., Jiang, C., Arneth, A., Georgievski, G., Li, W., Ceccherini, G., Anthoni, P., Lawrence, P., Wiltshire, A., Pongratz, J., Piao, S., Sitch, S., Goll, D. S., Arora, V. K., Lienert, S., Lombardozzi, D., Kato, E., Nabel, J. E. M. S., Tian, H., Friedlingstein, P., and Cescatti, A.: Increased control of
760 vegetation on global terrestrial energy fluxes, *Nature Climate Change*, 10, 356–362, <https://doi.org/10.1038/s41558-020-0717-0>, 2020.
- Frank, D., Reichstein, M., Bahn, M., Thonicke, K., Frank, D., Mahecha, M. D., Smith, P., van der Velde, M., Vicca, S., Babst, F., Beer, C., Buchmann, N., Canadell, J. G., Ciais, P., Cramer, W., Ibrom, A., Miglietta, F., Poulter, B., Rammig, A., Seneviratne, S. I., Walz, A., Wattenbach, M., Zavala, M. A., and Zscheischler, J.: Effects of climate extremes on the terrestrial carbon cycle: concepts, processes and potential future impacts, *Global Change Biology*, 21, 2861–2880, <https://doi.org/https://doi.org/10.1111/gcb.12916>, 2015.
- 765 Franz, M., Simpson, D., Arneth, A., and Zaehle, S.: Development and evaluation of an ozone deposition scheme for coupling to a terrestrial biosphere model, *Biogeosciences*, 14, 45–71, <https://doi.org/10.5194/bg-14-45-2017>, 2017.
- Fratini, G. and Mauder, M.: Towards a consistent eddy-covariance processing: an intercomparison of EddyPro and TK3, *Atmospheric Measurement Techniques*, 7, 2273–2281, <https://doi.org/10.5194/amt-7-2273-2014>, 2014.
- Friedlingstein, P., Jones, M. W., O’Sullivan, M., Andrew, R. M., Hauck, J., Peters, G. P., Peters, W., Pongratz, J., Sitch, S., Le Quéré, C.,
770 Bakker, D. C. E., Canadell, J. G., Ciais, P., Jackson, R. B., Anthoni, P., Barbero, L., Bastos, A., Bastrikov, V., Becker, M., Bopp, L., Buitenhuis, E., Chandra, N., Chevallier, F., Chini, L. P., Currie, K. I., Feely, R. A., Gehlen, M., Gilfillan, D., Gkritzalis, T., Goll, D. S., Gruber, N., Gutekunst, S., Harris, I., Haverd, V., Houghton, R. A., Hurtt, G., Ilyina, T., Jain, A. K., Joetzjer, E., Kaplan, J. O., Kato, E., Klein Goldewijk, K., Korsbakken, J. I., Landschützer, P., Lauvset, S. K., Lefèvre, N., Lenton, A., Lienert, S., Lombardozzi, D., Marland, G., McGuire, P. C., Melton, J. R., Metzl, N., Munro, D. R., Nabel, J. E. M. S., Nakaoka, S.-I., Neill, C., Omar, A. M., Ono, T., Peregon, A., Pierrot, D., Poulter, B., Rehder, G., Resplandy, L., Robertson, E., Rödenbeck, C., Séférian, R., Schwinger, J., Smith, N., Tans, P. P.,
775 Tian, H., Tilbrook, B., Tubiello, F. N., van der Werf, G. R., Wiltshire, A. J., and Zaehle, S.: Global Carbon Budget 2019, *Earth System Science Data*, 11, 1783–1838, <https://doi.org/10.5194/essd-11-1783-2019>, 2019.
- Friend, A., Stevens, A., Knox, R., and Cannell, M.: A process-based, terrestrial biosphere model of ecosystem dynamics (Hybrid v3.0), *Ecological Modelling*, 95, 249–287, [https://doi.org/10.1016/S0304-3800\(96\)00034-8](https://doi.org/10.1016/S0304-3800(96)00034-8), 1997.
- 780 Friend, A. D.: Modelling canopy CO₂ fluxes: are ‘big-leaf’ simplifications justified?, *Global ecology and biogeography: a journal of macroecology*, 10, 603–619, <https://nph.onlinelibrary.wiley.com/doi/abs/10.1046/j.1466-822x.2001.00268.x>, 2001.
- Friend, A. D.: Terrestrial plant production and climate change, *Journal of experimental botany*, 61, 1293–1309, 2010.
- Froelich, N., Croft, H., Chen, J. M., Gonsamo, A., and Staebler, R. M.: Trends of carbon fluxes and climate over a mixed temperate–boreal transition forest in southern Ontario, Canada, *Agricultural and Forest Meteorology*, 211, 72–84, 2015.
- 785 Fu, Y. H., Zhao, H., Piao, S., Peaucelle, M., Peng, S., Zhou, G., Ciais, P., Huang, M., Menzel, A., Peñuelas, J., Song, Y., Vitasse, Y., Zeng, Z., and Janssens, I. A.: Declining global warming effects on the phenology of spring leaf unfolding, *Nature*, 526, 104–107, <https://doi.org/10.1038/nature15402>, 2015.
- Gaumont-Guay, D., Black, T. A., Griffis, T. J., Barr, A. G., Jassal, R. S., and Nesic, Z.: Interpreting the dependence of soil respiration on soil temperature and water content in a boreal aspen stand, *Agricultural and Forest Meteorology*, 140, 220–235,
790 <https://doi.org/10.1016/j.agrformet.2006.08.003>, 2006.



- Gonsamo, A., Croft, H., Chen, J. M., Wu, C., Froelich, N., and Staebler, R. M.: Radiation contributed more than temperature to increased decadal autumn and annual carbon uptake of two eastern North America mature forests, *Agricultural and Forest Meteorology*, 201, 8–16, <https://doi.org/10.1016/j.agrformet.2014.11.007>, 2015.
- Gower, S. T., Kucharik, C. J., and Norman, J. M.: Direct and Indirect Estimation of Leaf Area Index, fAPAR, and Net Primary Production of Terrestrial Ecosystems, *Remote Sensing of Environment*, 70, 29–51, [https://doi.org/10.1016/S0034-4257\(99\)00056-5](https://doi.org/10.1016/S0034-4257(99)00056-5), 1999.
- Houborg, R., Cescatti, A., Migliavacca, M., and Kustas, W.: Satellite retrievals of leaf chlorophyll and photosynthetic capacity for improved modeling of GPP, *Agricultural and Forest Meteorology*, 177, 10–23, <https://doi.org/https://doi.org/10.1016/j.agrformet.2013.04.006>, 2013.
- Huntingford, C., Burke, E. J., Jones, C. D., Jeffers, E. S., and Wiltshire, A. J.: Nitrogen cycle impacts on CO₂ fertilisation and climate forcing of land carbon stores, *Environmental Research Letters*, 17, 044072, <https://doi.org/10.1088/1748-9326/ac6148>, 2022.
- Högberg, P., Näsholm, T., Franklin, O., and Högberg, M. N.: Tamm Review: On the nature of the nitrogen limitation to plant growth in Fennoscandian boreal forests, *Forest Ecology and Management*, 403, 161–185, <https://doi.org/10.1016/j.foreco.2017.04.045>, 2017.
- Jonard, M., Fürst, A., Verstraeten, A., Thimonier, A., Timmermann, V., Potočić, N., Waldner, P., Benham, S., Hansen, K., Merilä, P., Ponette, Q., de la Cruz, A. C., Roskams, P., Nicolas, M., Croisé, L., Ingerslev, M., Matteucci, G., Decinti, B., Bascietto, M., and Rautio, P.: Tree mineral nutrition is deteriorating in Europe, *Global Change Biology*, 21, 418–430, <https://doi.org/https://doi.org/10.1111/gcb.12657>, 2015.
- Kattge, J., Díaz, S., Lavorel, S., Prentice, I. C., Leadley, P., Bönisch, G., Garnier, E., Westoby, M., Reich, P. B., Wright, I. J., Cornelissen, J. H. C., Violle, C., Harrison, S. P., Van Bodegom, P. M., Reichstein, M., Enquist, B. J., Soudzilovskaia, N. A., Ackerly, D. D., Anand, M., Atkin, O., Bahn, M., Baker, T. R., Baldocchi, D., Bekker, R., Blanco, C. C., Blonder, B., Bond, W. J., Bradstock, R., Bunker, D. E., Casanoves, F., Caverner-Bares, J., Chambers, J. Q., Chapin III, F. S., Chave, J., Coomes, D., Cornwell, W. K., Craine, J. M., Dobrin, B. H., Duarte, L., Durka, W., Elser, J., Esser, G., Estiarte, M., Fagan, W. F., Fand, J., Fernández-Méndez, F., Fidelis, A., Finegan, B., Flores, O., Ford, H., Frank, D., Freschet, G. T., Fyllas, N. M., Gallagher, R. V., Green, W. A., Gutierrez, A. G., Thomas, H., Higgins, S. I., Hodgson, J. G., Jalili, A., Jansen, S., Joly, C. A., Kerkhoff, A. J., Kirkup, D., Kitajima, K., Kleyer, M., Klotz, S., Knops, J. M. H., Kramer, K., Kühn, I., Kurokawa, H., Laughlin, D., Lee, T. D., Leishman, M., Lens, F., Lenz, T., Lewis, S. L., Lloyd, J., Llusà, J., Louault, F., Ma, S., Mahecha, M. D., Manning, P., Massad, T., Medlyn, B. E., Messier, J., Moles, A. T., Müller, S. C., Nadrowski, K., Naeem, S., Niinemets, Ü., Nöllert, S., Nüske, A., Ogaya, R., Oleksyn, J., Onipchenko, V. G., Onoda, Y., Ordoñez, J., Overbeck, G., Ozinga, W. A., Patino, S., Paula, S., Pausas, J. G., Peñuelas, J., Phillips, O. L., Pillar, V., Poorter, H., Poorter, L., Poschlod, P., Prinzing, A., Proulx, R., Rammig, A., Reinsch, S., Reu, B., Sack, L., Salgado-Negret, B., Sardans, J., Shiodera, S., Shipley, B., Siefert, A., Sosinski, E., Soussana, J. F., Swaine, E., Swenson, N., Thompson, K., Thornton, P., Waldram, M., Weiher, E., White, M., White, S., Wright, S. J., Yguel, B., Zaehle, S., Zanne, A. E., and Wirth, C.: TRY - a global database of plant traits, *Global Change Biology*, 17, 2905–2935, 2011.
- Kirschbaum, M.: The temperature dependence of organic-matter decomposition—still a topic of debate, *Soil Biology and Biochemistry*, 38, 2510–2518, <https://doi.org/10.1016/j.soilbio.2006.01.030>, 2006.
- Kou-Giesbrecht, S., Arora, V. K., Seiler, C., Arneth, A., Falk, S., Jain, A. K., Joos, F., Kennedy, D., Knauer, J., Sitch, S., O’Sullivan, M., Pan, N., Sun, Q., Tian, H., Vuichard, N., and Zaehle, S.: Evaluating nitrogen cycling in terrestrial biosphere models: a disconnect between the carbon and nitrogen cycles, *Earth System Dynamics*, 14, 767–795, <https://doi.org/10.5194/esd-14-767-2023>, 2023.
- Krinner, G., Viovy, N., de Noblet-Ducoudré, N., Ogée, J., Polcher, J., Friedlingstein, P., Ciais, P., Sitch, S. A., and Prentice, I. C.: A dynamic global vegetation model for studies of the coupled atmosphere-biosphere system, *Global Biogeochemical Cycles*, 19, GB1015, 2005.
- Kull, O. and Kruijt, B.: Leaf photosynthetic light response: a mechanistic model for scaling photosynthesis to leaves and canopies, *Functional Ecology*, 12, 767–777, 1998.



- Lamarque, J.-F., Bond, T. C., Eyring, V., Granier, C., Heil, A., Klimont, Z., Lee, D., Lioussé, C., Mieville, A., Owen, B., Schultz, M. G., Shindell, D., Smith, S. J., Stehfest, E., Van Aardenne, J., Cooper, O. R., Kainuma, M., Mahowald, N., McConnell, J. R., Naik, V., Riahi, K., and van Vuuren, D. P.: Historical (1850–2000) gridded anthropogenic and biomass burning emissions of reactive gases and aerosols: methodology and application, *Atmospheric Chemistry and Physics*, 10, 7017–7039, <https://doi.org/10.5194/acp-10-7017-2010>, 2010.
- Lamarque, J.-F., Kyle, G. P., Meinshausen, M., Riahi, K., Smith, S. J., van Vuuren, D. P., Conley, A. J., and Vitt, F.: Global and regional evolution of short-lived radiatively-active gases and aerosols in the Representative Concentration Pathways, *Climatic Change*, 109, 191, <https://doi.org/10.1007/s10584-011-0155-0>, 2011.
- LeBauer, D. S. and Treseder, K. K.: Nitrogen limitation of net primary productivity in terrestrial ecosystems is globally distributed, *Ecology*, 89, 371–379, <https://doi.org/10.1890/06-2057.1>, 2008.
- Lee, X., Fuentes, J. D., Staebler, R. M., and Neumann, H. H.: Long-term observation of the atmospheric exchange of CO₂ with a temperate deciduous forest in southern Ontario, Canada, *Journal of Geophysical Research: Atmospheres*, 104, 15 975–15 984, <https://doi.org/https://doi.org/10.1029/1999JD900227>, 1999.
- Liu, W., Zhang, Z., and Wan, S.: Predominant role of water in regulating soil and microbial respiration and their responses to climate change in a semiarid grassland, *Global Change Biology*, 15, 184–195, <https://doi.org/https://doi.org/10.1111/j.1365-2486.2008.01728.x>, 2009.
- Loescher, H. W., Law, B. E., Mahrt, L., Hollinger, D. Y., Campbell, J., and Wofsy, S. C.: Uncertainties in, and interpretation of, carbon flux estimates using the eddy covariance technique, *Journal of Geophysical Research: Atmospheres*, 111, 2005JD006 932, <https://doi.org/10.1029/2005JD006932>, 2006.
- Lombardozi, D., Levis, S., Bonan, G., and Sparks, J. P.: Predicting photosynthesis and transpiration responses to ozone: decoupling modeled photosynthesis and stomatal conductance, *Biogeosciences*, 9, 3113–3130, <https://doi.org/10.5194/bg-9-3113-2012>, 2012.
- Lombardozi, D., Sparks, J. P., and Bonan, G.: Integrating O₃ influences on terrestrial processes: photosynthetic and stomatal response data available for regional and global modeling, *Biogeosciences*, 10, 6815–6831, <https://doi.org/10.5194/bg-10-6815-2013>, 2013.
- Lombardozi, D., Levis, S., Bonan, G., Hess, P. G., and Sparks, J. P.: The Influence of Chronic Ozone Exposure on Global Carbon and Water Cycles, *Journal of Climate*, 28, 292–305, <https://doi.org/10.1175/JCLI-D-14-00223.1>, 2015.
- Lu, X., Croft, H., Chen, J. M., Luo, Y., and Ju, W.: Estimating photosynthetic capacity from optimized Rubisco–chlorophyll relationships among vegetation types and under global change, *Environmental Research Letters*, 17, 014 028, 2022.
- Luo, X., Croft, H., Chen, J. M., Bartlett, P., Staebler, R., and Froelich, N.: Incorporating leaf chlorophyll content into a two-leaf terrestrial biosphere model for estimating carbon and water fluxes at a forest site, *Agricultural and Forest Meteorology*, 248, 156–168, 2018.
- Medlyn, B. E., Duursma, R. A., Eamus, D., Ellsworth, D. S., Prentice, I. C., Barton, C. V. M., Crous, K. Y., De Angelis, P., Freeman, M., and Wingate, L.: Reconciling the optimal and empirical approaches to modelling stomatal conductance, *Global Change Biology*, 17, 2134–2144, <https://doi.org/https://doi.org/10.1111/j.1365-2486.2010.02375.x>, 2011.
- Medlyn, B. E., Zaehle, S., De Kauwe, M. G., Walker, A. P., Dietze, M. C., Hanson, P. J., Hickler, T., Jain, A. K., Luo, Y., Parton, W., Prentice, I. C., Thornton, P. E., Wang, S., Wang, Y.-P., Weng, E., Iversen, C. M., McCarthy, H. R., Warren, J. M., Oren, R., and Norby, R. J.: Using ecosystem experiments to improve vegetation models, *Nature Climate Change*, 5, 528–534, <https://doi.org/10.1038/nclimate2621>, 2015.
- Meyerholt, J., Zaehle, S., and Smith, M. J.: Variability of projected terrestrial biosphere responses to elevated levels of atmospheric CO₂ due to uncertainty in biological nitrogen fixation, *Biogeosciences*, 13, 1491–1518, 2016.
- Meyerholt, J., Sickel, K., and Zaehle, S.: Ensemble projections elucidate effects of uncertainty in terrestrial nitrogen limitation on future carbon uptake, *Global Change Biology*, 26, 3978–3996, <https://doi.org/https://doi.org/10.1111/gcb.15114>, 2020a.



- 865 Meyerholt, J., Sickel, K., and Zaehle, S.: Ensemble projections elucidate effects of uncertainty in terrestrial nitrogen limitation on future carbon uptake, *Global Change Biology*, 26, 3978–3996, <https://doi.org/10.1111/gcb.15114>, 2020b.
- Miller, J.: A formula for average foliage density, *Australian Journal of Botany*, 15, 141–144, 1967.
- Muñoz Sabater, J., Dutra, E., Agustí-Panareda, A., Albergel, C., Arduini, G., Balsamo, G., Boussetta, S., Choulga, M., Harrigan, S., Hersbach, H., Martens, B., Miralles, D. G., Piles, M., Rodríguez-Fernández, N. J., Zsoter, E., Buontempo, C., and Thépaut, J.-N.: ERA5-Land: a
870 state-of-the-art global reanalysis dataset for land applications, *Earth System Science Data*, 13, 4349–4383, <https://doi.org/10.5194/essd-13-4349-2021>, 2021.
- Neumann, H., Den Hartog, G., and Shaw, R.: Leaf area measurements based on hemispheric photographs and leaf-litter collection in a deciduous forest during autumn leaf-fall, *Agricultural and Forest Meteorology*, 45, 325–345, [https://doi.org/10.1016/0168-1923\(89\)90052-X](https://doi.org/10.1016/0168-1923(89)90052-X), 1989.
- 875 Niinemets, Ü., Kull, O., and Tenhunen, J. D.: An analysis of light effects on foliar morphology, physiology, and light interception in temperate deciduous woody species of contrasting shade tolerance, *Tree Physiology*, 18, 681–696, <https://doi.org/10.1093/treephys/18.10.681>, 1998.
- Niinemets, Ü., Keenan, T. F., and Hallik, L.: A worldwide analysis of within-canopy variations in leaf structural, chemical and physiological traits across plant functional types, *New Phytologist*, 205, 973–993, 2015.
- Novak, K., Schaub, M., Fuhrer, J., Skelly, J., Hug, C., Landolt, W., Bleuler, P., and Kräuchi, N.: Seasonal trends in reduced leaf
880 gas exchange and ozone-induced foliar injury in three ozone sensitive woody plant species, *Environmental Pollution*, 136, 33–45, <https://doi.org/https://doi.org/10.1016/j.envpol.2004.12.018>, 2005.
- Oe, Y., Yamamoto, A., and Mariko, S.: Characteristics of soil respiration temperature sensitivity in a *Pinus/Betula* mixed forest during periods of rising and falling temperatures under the Japanese monsoon climate, *Journal of Ecology and Environment*, 34, 193–202, <https://doi.org/10.5141/JEFB.2011.021>, 2011.
- 885 Orchard, V. A. and Cook, F.: Relationship between soil respiration and soil moisture, *Soil Biology and Biochemistry*, 15, 447–453, [https://doi.org/https://doi.org/10.1016/0038-0717\(83\)90010-X](https://doi.org/https://doi.org/10.1016/0038-0717(83)90010-X), 1983.
- O’Sullivan, M., Friedlingstein, P., Sitch, S., Anthoni, P., Arneth, A., Arora, V. K., Bastrikov, V., Delire, C., Goll, D. S., Jain, A., Kato, E., Kennedy, D., Knauer, J., Lienert, S., Lombardozzi, D., McGuire, P. C., Melton, J. R., Nabel, J. E. M. S., Pongratz, J., Poulter, B., Séférian, R., Tian, H., Vuichard, N., Walker, A. P., Yuan, W., Yue, X., and Zaehle, S.: Process-oriented analysis of dominant sources of uncertainty
890 in the land carbon sink, *Nature Communications*, 13, <https://doi.org/10.1038/s41467-022-32416-8>, 2022.
- Parton, W. J., Scurlock, J. M. O., Ojima, D. S., Gilmanov, T. G., Scholes, R. J., Schimmel, D. S., Kirchner, T., Menaut, J. C., Seastedt, T., Moya, E. G., Kamnalrut, A., and Kinyamario, J. I.: Observations and modelling of biomass and soil organic matter dynamics for the grassland biome worldwide, *Global Biogeochemical Cycles*, 7, 785–809, 1993.
- Piao, S., Liu, Q., Chen, A., Janssens, I. A., Fu, Y., Dai, J., Liu, L., Lian, X., Shen, M., and Zhu, X.: Plant phenology and global climate
895 change: Current progresses and challenges, *Global Change Biology*, 25, 1922–1940, <https://doi.org/10.1111/gcb.14619>, 2019a.
- Piao, S., Zhang, X., Chen, A., Liu, Q., Lian, X., Wang, X., Peng, S., and Wu, X.: The impacts of climate extremes on the terrestrial carbon cycle: A review, *Science China Earth Sciences*, 62, 1551–1563, <https://doi.org/10.1007/s11430-018-9363-5>, 2019b.
- Richardson, A. D., Keenan, T. F., Migliavacca, M., Ryu, Y., Sonnentag, O., and Toomey, M.: Climate change, phenology, and phenological control of vegetation feedbacks to the climate system, *Agricultural and Forest Meteorology*, 169, 156–173,
900 <https://doi.org/https://doi.org/10.1016/j.agrformet.2012.09.012>, 2013.
- Rogers, A., Medlyn, B. E., Dukes, J. S., Bonan, G., Von Caemmerer, S., Dietze, M. C., Kattge, J., Leakey, A. D., Mercado, L. M., Niinemets, Ü., et al.: A roadmap for improving the representation of photosynthesis in Earth system models, *New Phytologist*, 213, 22–42, 2017.



- Rogers, C., Chen, J. M., Croft, H., Gonsamo, A., Luo, X., Bartlett, P., and Staebler, R. M.: Daily leaf area index from photosynthetically active radiation for long term records of canopy structure and leaf phenology, *Agricultural and Forest Meteorology*, 304, 108407, 2021.
- 905 Ruehr, N. K., Martin, J. G., and Law, B. E.: Effects of water availability on carbon and water exchange in a young ponderosa pine forest: Above- and belowground responses, *Agricultural and Forest Meteorology*, 164, 136–148, <https://doi.org/https://doi.org/10.1016/j.agrformet.2012.05.015>, 2012.
- Schwalm, C. R., Williams, C. A., Schaefer, K., Arneth, A., Bonal, D., Buchmann, N., Chen, J., Law, B. E., Lindroth, A., Luyssaert, S., Reichstein, M., and Richardson, A. D.: Assimilation exceeds respiration sensitivity to drought: A FLUXNET synthesis, *Global Change*
910 *Biology*, 16, 657–670, <https://doi.org/https://doi.org/10.1111/j.1365-2486.2009.01991.x>, 2010.
- Simpson, D., Arneth, A., Mills, G., Solberg, S., and Uddling, J.: Ozone — the persistent menace: interactions with the N cycle and climate change, *Current Opinion in Environmental Sustainability*, 9-10, 9–19, <https://doi.org/https://doi.org/10.1016/j.cosust.2014.07.008>, sI: System dynamics and sustainability, 2014.
- Sims, D. A. and Gamon, J. A.: Relationships between leaf pigment content and spectral reflectance across a wide range of species, leaf
915 structures and developmental stages, *Remote Sensing of Environment*, 81, 337–354, [https://doi.org/10.1016/S0034-4257\(02\)00010-X](https://doi.org/10.1016/S0034-4257(02)00010-X), 2002.
- Sokolov, A. P., Kicklighter, D. W., Melillo, J. M., Felzer, B. S., Schlosser, C. A., and Cronin, T. W.: Consequences of Considering Carbon–Nitrogen Interactions on the Feedbacks between Climate and the Terrestrial Carbon Cycle, *Journal of Climate*, 21, 3776–3796, <https://doi.org/10.1175/2008JCLI2038.1>, 2008.
- 920 Spitters, C. J. T.: Separating the Diffuse and Direct Component of Global Radiation and Its Implications for Modeling Canopy Photosynthesis .2. Calculation of Canopy Photosynthesis, *Agricultural and Forest Meteorology*, 38, 231–242, 1986.
- Sun, Y., Gu, L., Wen, J., van der Tol, C., Porcar-Castell, A., Joiner, J., Chang, C. Y., Magney, T., Wang, L., Hu, L., Rascher, U., Zarco-Tejada, P., Barrett, C. B., Lai, J., Han, J., and Luo, Z.: From remotely sensed solar-induced chlorophyll fluorescence to ecosystem structure, function, and service: Part I—Harnessing theory, *Global Change Biology*, 29, 2926–2952, <https://doi.org/https://doi.org/10.1111/gcb.16634>,
925 2023.
- Teklemariam, T., Staebler, R., and Barr, A.: Eight years of carbon dioxide exchange above a mixed forest at Borden, Ontario, *Agricultural and Forest Meteorology*, 149, 2040–2053, 2009.
- Thomas, R. Q., Zaehle, S., Templer, P. H., and Goodale, C. L.: Global patterns of nitrogen limitation: confronting two global biogeochemical models with observations, *Global Change Biology*, 19, 2986–2998, <https://doi.org/10.1111/gcb.12281>, 2013.
- 930 Thomas, R. Q., Brookshire, E. N. J., and Gerber, S.: Nitrogen limitation on land: how can it occur in Earth system models?, *Global Change Biology*, 21, 1777–1793, <https://doi.org/https://doi.org/10.1111/gcb.12813>, 2015.
- Thornton, P. E., Lamarque, J.-F., Rosenbloom, N. A., and Mahowald, N. M.: Influence of carbon-nitrogen cycle coupling on land model response to CO₂ fertilization and climate variability, *Global Biogeochemical Cycles*, 21, <https://doi.org/https://doi.org/10.1029/2006GB002868>, 2007.
- 935 Thornton, P. E., Doney, S. C., Lindsay, K., Moore, J. K., Mahowald, N., Randerson, J. T., Fung, I., Lamarque, J.-F., Feddes, J. J., and Lee, Y.-H.: Carbon-nitrogen interactions regulate climate-carbon cycle feedbacks: results from an atmosphere-ocean general circulation model, *Biogeosciences*, 6, 2099–2120, <https://doi.org/10.5194/bg-6-2099-2009>, 2009.
- Thum, T., Caldararu, S., Engel, J., Kern, M., Pallandt, M., Schnur, R., Yu, L., and Zaehle, S.: A new model of the coupled carbon, nitrogen, and phosphorus cycles in the terrestrial biosphere (QUINCY v1. 0; revision 1996), *Geoscientific Model Development*, 12, 4781–4802,
940 2019.



- van der Molen, M., Dolman, A., Ciais, P., Eglin, T., Gobron, N., Law, B., Meir, P., Peters, W., Phillips, O., Reichstein, M., Chen, T., Dekker, S., Doubkova, M., Friedl, M., Jung, M., van den Hurk, B., de Jeu, R., Kruijt, B., Ohta, T., Rebel, K., Plummer, S., Seneviratne, S., Sitch, S., Teuling, A., van der Werf, G., and Wang, G.: Drought and ecosystem carbon cycling, *Agricultural and Forest Meteorology*, 151, 765–773, <https://doi.org/https://doi.org/10.1016/j.agrformet.2011.01.018>, 2011.
- 945 von Buttlar, J., Zscheischler, J., Rammig, A., Sippel, S., Reichstein, M., Knohl, A., Jung, M., Menzer, O., Arain, M. A., Buchmann, N., Cescatti, A., Gianelle, D., Kiely, G., Law, B. E., Magliulo, V., Margolis, H., McCaughey, H., Merbold, L., Migliavacca, M., Montagnani, L., Oechel, W., Pavelka, M., Peichl, M., Rambal, S., Raschi, A., Scott, R. L., Vaccari, F. P., van Gorsel, E., Varlagin, A., Wohlfahrt, G., and Mahecha, M. D.: Impacts of droughts and extreme-temperature events on gross primary production and ecosystem respiration: a systematic assessment across ecosystems and climate zones, *Biogeosciences*, 15, 1293–1318, <https://doi.org/10.5194/bg-15-1293-2018>,
950 2018.
- Walker, A. P., Beckerman, A. P., Gu, L., Kattge, J., Cernusak, L. A., Domingues, T. F., Scales, J. C., Wohlfahrt, G., Wullschleger, S. D., and Woodward, F. I.: The relationship of leaf photosynthetic traits – V_{cmax} and J_{max} – to leaf nitrogen, leaf phosphorus, and specific leaf area: a meta-analysis and modeling study, *Ecology and Evolution*, 4, 3218–3235, <https://doi.org/https://doi.org/10.1002/ece3.1173>, 2014.
- Walker, A. P., De Kauwe, M. G., Bastos, A., Belmecheri, S., Georgiou, K., Keeling, R. F., McMahon, S. M., Medlyn, B. E., Moore, D.
955 J. P., Norby, R. J., Zaehle, S., Anderson-Teixeira, K. J., Battipaglia, G., Brienen, R. J. W., Cabugao, K. G., Cailleret, M., Campbell, E., Canadell, J. G., Ciais, P., Craig, M. E., Ellsworth, D. S., Farquhar, G. D., Fatichi, S., Fisher, J. B., Frank, D. C., Graven, H., Gu, L., Haverd, V., Heilman, K., Heimann, M., Hungate, B. A., Iversen, C. M., Joos, F., Jiang, M., Keenan, T. F., Knauer, J., Körner, C., Leshyk, V. O., Leuzinger, S., Liu, Y., MacBean, N., Malhi, Y., McVicar, T. R., Penuelas, J., Pongratz, J., Powell, A. S., Riutta, T., Sabot, M. E. B., Schleucher, J., Sitch, S., Smith, W. K., Sulman, B., Taylor, B., Terrer, C., Torn, M. S., Treseder, K. K., Trugman, A. T., Trumbore, S. E.,
960 van Mantgem, P. J., Voelker, S. L., Whelan, M. E., and Zuidema, P. A.: Integrating the evidence for a terrestrial carbon sink caused by increasing atmospheric CO₂, *New Phytologist*, 229, 2413–2445, <https://doi.org/https://doi.org/10.1111/nph.16866>, 2021.
- Wellburn, A. R.: The Spectral Determination of Chlorophylls a and b, as well as Total Carotenoids, Using Various Solvents with Spectrophotometers of Different Resolution, *Journal of Plant Physiology*, 144, 307–313, [https://doi.org/https://doi.org/10.1016/S0176-1617\(11\)81192-2](https://doi.org/https://doi.org/10.1016/S0176-1617(11)81192-2), 1994.
- 965 Wullschleger, S. D.: Biochemical Limitations to Carbon Assimilation in C₃ Plants—A Retrospective Analysis of the A/C_i Curves from 109 Species, *Journal of experimental botany*, 44, 907–920, <https://doi.org/10.1093/jxb/44.5.907>, 1993.
- Yu, L., Ahrens, B., Wutzler, T., Schrumpf, M., and Zaehle, S.: Jena Soil Model (JSM v1.0; revision 1934): a microbial soil organic carbon model integrated with nitrogen and phosphorus processes, *Geoscientific Model Development*, 13, 783–803, <https://doi.org/10.5194/gmd-13-783-2020>, 2020.
- 970 Yu, X., Orth, R., Reichstein, M., Bahn, M., Klosterhalfen, A., Knohl, A., Koepsch, F., Migliavacca, M., Mund, M., Nelson, J. A., Stocker, B. D., Walther, S., and Bastos, A.: Contrasting drought legacy effects on gross primary productivity in a mixed versus pure beech forest, *Biogeosciences*, 19, 4315–4329, <https://doi.org/10.5194/bg-19-4315-2022>, 2022.
- Zaehle, S.: Terrestrial nitrogen–carbon cycle interactions at the global scale, *Philosophical Transactions of the Royal Society B: Biological Sciences*, 368, 20130 125, 2013.
- 975 Zaehle, S. and Dalmonech, D.: Carbon–nitrogen interactions on land at global scales: current understanding in modelling climate biosphere feedbacks, *Current Opinion in Environmental Sustainability*, 3, 311–320, 2011.
- Zaehle, S. and Friend, A.: Carbon and nitrogen cycle dynamics in the O-CN land surface model: 1. Model description, site-scale evaluation, and sensitivity to parameter estimates, *Global Biogeochemical Cycles*, 24, 2010.



- 980 Zaehle, S., Ciais, P., Friend, A. D., and Prieur, V.: Carbon benefits of anthropogenic reactive nitrogen offset by nitrous oxide emissions, *Nature Geoscience*, 4, 601–605, 2011.
- Zhang, Q., Phillips, R. P., Manzoni, S., Scott, R. L., Oishi, A. C., Finzi, A., Daly, E., Vargas, R., and Novick, K. A.: Changes in photosynthesis and soil moisture drive the seasonal soil respiration-temperature hysteresis relationship, *Agricultural and Forest Meteorology*, 259, 184–195, <https://doi.org/10.1016/j.agrformet.2018.05.005>, 2018.